Núcleo de Investigação em Políticas Económicas e Empresariais

#13
2023

WORKING PAPER

Susana Campos-Martins

Cristina Amado

"Modelling causality in nonstationary variances with an application to carbon markets"

https://nipe.eeg.uminho.pt/

«This paper is financed by National Funds of the FCT – Portuguese Foundation for Science and Technology within the project «UIDB/03182/2020»

Universidade do Minho
Escola de Economia e Gestão

Modelling causality in nonstationary variances with an application to carbon markets*

Susana Campos-Martins†
Católica Lisbon School of Business & Economics

Cristina Amado‡
University of Minho and NIPE

December 12, 2023

Abstract

In this paper we propose a multivariate generalisation of the multiplicative decomposition of the volatility within the class of conditional correlation GARCH models. The GARCH variance equations are multiplicatively decomposed into a deterministic nonstationary component describing the long-run movements in volatility and a short-run dynamic component allowing for volatility spillover effects across markets or assets. The conditional correlations are assumed to be time-invariant in its simplest form or generalised into a flexible dynamic parameterisation. Parameters of the model are estimated equation-by-equation by maximum likelihood applying the maximisation by parts algorithm to the variance equations, and thereafter to the structure of conditional correlations. An empirical application using carbon markets data illustrates the usefulness of the model. Our results suggest that, after modelling the variance equations accordingly, we find evidence that the transmission mechanism of shocks persists which is supported by the presence of variance interactions robust to nonstationarity.

Keywords: Variance interactions; Nonstationarity; Short- and long-term volatility; Lagrange multiplier test.

JEL classification: C12, C13, C32, C51.

* **Acknowledgments:** This paper is financed by National Funds of the FCT Portuguese Foundation for Science and Technology within the project UIDB/03182/2020. This work has also been supported by funding from COMPETE (Ref. No. POCI-01-0145-FEDER-028234), with the FCT/MEC's financial support through national funding and by the ERDF through the Operational Programme on "Competitiveness and Internationalization" - COMPETE 2020 under the PT2020 Partnership Agreement. The first author wishes to acknowledge the financial support from the Portuguese Foundation for Science and Technology under the Doctoral scholarship SFRH/BD/109539/2015. Part of this work was carried out when the first author was visiting New York University Stern School of Business hosted by Robert F. Engle. The authors wish to thank participants of the 21st Dynamic Econometrics Conference, Washington D.C., March 2019; 12th Annual Society for Financial Econometrics (SoFiE) Conference, Shanghai, June 2019; Asian Meeting of the Econometric Society, Xiamen, June 2019; 28th Annual European Financial Management Association Annual Meeting, Azores, June 2019; 13th Annual Meeting of the Portuguese Economic Journal in Évora, July 2019; IV Econometric Models of Climate Change Conference, Milan, August 2019; 18th International Conference on Credit Risk Evaluation Designed for Institutional Targeting in Finance - Assessing and Managing Climate Change Risk: Opportunities for Financial Institutions, Venice, September 2019; 4th International Workshop in Financial Econometrics in Maceió, October 2019; 33rd $(EC)^2$ Conference on Econometrics of High Frequency Data & Factor Models, Paris, December 2022; and in seminars at New York University Stern School of Business, New York City, February 2019, University of Minho, School of Economics and Management, Braga, April 2019, and University Carlos III Madrid, Department of Statistics, February 2023. The responsibility for any errors and shortcomings in this paper remains ours.

† Católica Lisbon School of Business & Economics, Palma de Cima, 1649-023 Lisbon, Portugal; e-mail address: scmartins@ucp.pt.

‡ Corresponding author: Department of Economics and NIPE, University of Minho, Campus de Gualtar, 4710-057 Braga, Portugal; e-mail address: camado@eeg.uminho.pt.

1 Introduction

The class of conditional correlation generalized autoregressive conditional heteroskedasticity (CC-GARCH) models introduced by Bollerslev (1990) has become a useful tool for modelling and forecasting (short-run) volatility and correlations between financial time series. In these models, the conditional variances are usually driven only by own past squared innovations and by own past conditional variances. As a result of international financial integration, because of the presence of information transmission, such structure may be insufficient to capture the time dependence in the data. In the presence of financial market interdependence, interactions in volatility also play an important role to earn knowledge on how information is transmitted across assets or markets. Empirical studies providing evidence for volatility spillovers include Baillie and Bollerslev (1990), King and Wadhwani (1990), Hamao, Masulis, and Ng (1990), Cifarelli and Paladino (2005) and Hong (2001), among others.

In this context, several specification techniques have been employed in the literature for examining volatility transmission mechanism spillovers. An interesting extension to the constant CC-GARCH (CCC-GARCH) model of Bollerslev (1990) that builds on the assumption of time-invariant correlations allowing dynamic volatility interactions in the form of cross-market ARCH and GARCH effects was introduced by Jeantheau (1998) and termed extended (E)CCC-GARCH model by He and Teräsvirta (2004). Other CC-GARCH models allowing for a volatility transmission structure include the vector autoregressive moving average (ARMA-)GARCH of Ling and McAleer (2003), the unrestricted ECCC-GARCH model of Conrad and Karanasos (2010) that allows for volatility feedback of either positive or negative sign and extensions thereafter on Karanasos, Paraskevopoulos, Ali, Karoglou, and Yfanti (2014), Conrad and Karanasos (2015) and Karanasos, Ali, Margaronis, and Nath (2018).

Yet evidence of volatility spillover effects can be due to neglected deterministic changes in the unconditional variance of long return series. Ewing and Malik (2005) documented that the statistical significance of volatility spillovers across assets or markets can be due to an inaccurate measurement of persistence in volatility. They report that accounting for regime shifts in volatility reduces remarkably the transmission of conditional variances and essentially removes the spillover effects. Therefore, ignoring variance nonstationarity, a feature usually observed in long time series as the result of structural changes in the unconditional variance, can lead to spurious volatility transmission as shown recently through Monte Carlo simulations by Caporin and Malik (2020). Since volatility shifts are often expected in long return series due to political, social or economic events, careful modelling of changes in the unconditional variance is therefore needed prior to modelling volatility spillover effects.

In this paper, we build on a generalisation of the multivariate multiplicative time-varying GARCH model of Amado and Teräsvirta (2014) and Silvennoinen and Teräsvirta (2021). The new model extends the family of conditional correlation GARCH models along two dimensions: it accounts for potential nonstationarity in volatility and it allows for interdependence in volatility. This is done by augmenting the conditional variance equations multiplicatively by a time-dependent component and extend it to the vector case where volatility interactions are allowed into the model. The structure of the conditional correlation matrix is assumed to be either time independent or to vary over time. Other multivariate generalisations of the time-varying GARCH model with multiplicative decomposition exist in the literature, but although these models are adequate for accounting nonstationarity in volatility, the ARCH and GARCH matrices are usually assumed to be diagonal and therefore variance spillovers are excluded from the model. Earlier examples include the local dynamic conditional correlation model by Feng (2006), the dynamic conditional correlation with mixed data sampling (DCC-MIDAS) model by Colacito, Engle, and Ghysels (2011) and the multiplicative DCC-GARCH model by Bauwens, Hafner, and Pierret (2013), among others.

We further develop a coherent modelling strategy equation by equation based on statistical inference. The algorithm is constructed to circumvent the curse of dimensionality and avoiding estimating unnecessary parameters. Our modelling building approach proceeds from specific-to-general and relies on statistical inference to the problem of specifying the model. Therefore, testing the assumptions of constant unconditional variance and no volatility spillovers is an important specification tool for building the model. As a misspecification test we propose a Lagrange Multiplier (LM) test for the presence of volatility interactions under nonstationarity in variance. A regression-based version of our test makes it straightforward to implement. Monte Carlo experiments show that the test performs reasonably well in small samples.

An empirical example to carbon markets data demonstrates the practical usefulness of the new model. The application shows how the specification yields useful information on the volatility dynamics and volatility interaction between the return series. Our model is applied to daily returns of carbon emissions futures and media-based climate concerns index. The results of the specification strategy strongly support the presence of smooth changes in the baseline volatility of processes and volatility transmission from one to another series in both applications. Interestingly, our findings suggest that if the nonstationary component of the variance was left unmodelled we would find no supporting statistical evidence for causality in variance.

The remainder of this paper is organized as follows. In Section 2 we present the new conditional correlation GARCH model with a detailed description of its variance and correlation components. Sections 3 and 4 are devoted to the estimation of parameters and to model specification, respectively. Section 5 introduces the LM test for volatility interactions. Section 6 contains Monte Carlo experiments of the finite sample properties of the test statistic. The empirical application to carbon markets data is provided in Section 7. Section 8 concludes the paper. A separate file contains supplementary material including another empirical example to four major spot exchange rates to illustrate the usefulness of our procedure.

2 The model

The model considered in this work belongs to the class of multivariate conditional correlation GARCH models introduced by Bollerslev (1990). The new model extends the original model by introducing nonstationarity and cross-asset (or cross-market) conditional heteroskedasticity in the conditional variance components and potentially time-varying correlations described by parametric extensions of the constant conditional correlation matrix. The model is an extension of the nonstationary parameterization introduced by Amado and Teräsvirta (2014) allowing for the presence of volatility transmission across assets or markets where past information of squared returns of all components are useful in predicting the variance process of any component. The proposed new class of models shall be named as multiplicative time-varying extended conditional correlation GARCH (MTV-ECC-GARCH) models. In order to present the model we introduce some notation. Let the stochastic vector process for the m-dimensional vector of returns be defined as

$$\mathbf{y}_t = \mathsf{E}(\mathbf{y}_t|\mathcal{F}_{t-1}) + \boldsymbol{\varepsilon}_t, \quad t = 1, \ldots, T, \tag{1}$$

where $\mathcal{F}_{t-1} = \sigma\{\boldsymbol{\varepsilon}_u : u < t\}$ is the σ-field generated by past values of $\boldsymbol{\varepsilon}_t$ and, for simplicity, the conditional expectation of the returns $\mathsf{E}(\mathbf{y}_t|\mathcal{F}_{t-1}) = \mathbf{0}$. Define the m-dimensional vector of innovations $\{\boldsymbol{\varepsilon}_t\}$ to have the multiplicative decomposition

$$\boldsymbol{\varepsilon}_t = \mathbf{S}_t\mathbf{D}_t\mathbf{z}_t = \boldsymbol{\Sigma}_t^{1/2}\mathbf{z}_t \tag{2}$$

where $\mathbf{S}_t = \mathsf{diag}(g_{1t}^{1/2}, \ldots, g_{mt}^{1/2})$ is a diagonal matrix of positive-valued deterministic functions of time and $\mathbf{D}_t = \mathsf{diag}(h_{1t}^{1/2}, \ldots, h_{mt}^{1/2})$ is a diagonal matrix of (weakly stationary) conditional standard deviations. The vector of errors $\mathbf{z}_t = (z_{1t}, \ldots, z_{mt})'$ form a sequence of random variables with $\mathsf{E}\mathbf{z}_t = \mathbf{0}$ and a positive definite time-varying covariance matrix $\mathsf{cov}(\mathbf{z}_t) = \mathbf{P}_t$, where $\mathbf{P}_t = [\rho_{ijt}]$, such that $\rho_{iit} = 1$ and $\rho_{ijt} \neq 0$, $i, j = 1, \ldots, m$. Assuming nonsingularity of $\mathsf{diag}(\boldsymbol{\Sigma}_t)$, we define the vector $\mathbf{z}_t = \mathbf{D}_t^{-1}\boldsymbol{\phi}_t = (\phi_{1t}/h_{1t}^{1/2}, \ldots, \phi_{mt}/h_{mt}^{1/2})'$, where the elements of $\boldsymbol{\phi}_t = (\varepsilon_{1t}/g_{1t}^{1/2}, \ldots, \varepsilon_{mt}/g_{mt}^{1/2})'$ are assumed to have a weakly stationary vector GARCH representation augmented with cross-asset (or cross-market) conditional heteroskedastic effects and conditional covariance matrix $\mathsf{E}(\boldsymbol{\phi}_t\boldsymbol{\phi}_t'|\mathcal{F}_{t-1}) = \mathbf{D}_t\mathbf{P}_t\mathbf{D}_t$. Furthermore, the vector of standardised errors $\boldsymbol{\zeta}_t = \mathbf{P}_t^{-1/2}\mathbf{z}_t \sim iid(\mathbf{0}, \mathbf{I}_m)$. From (2) it follows that

$$\mathsf{E}(\boldsymbol{\varepsilon}_t|\mathcal{F}_{t-1}) = \mathbf{0} \tag{3}$$

$$\mathsf{E}(\boldsymbol{\varepsilon}_t\boldsymbol{\varepsilon}_t'|\mathcal{F}_{t-1}) = \mathbf{S}_t\mathbf{D}_t\mathbf{P}_t\mathbf{D}_t\mathbf{S}_t = \boldsymbol{\Sigma}_t \tag{4}$$

where the conditional covariance matrix $\mathbf{\Sigma}_t = [\sigma_{ijt}]$ of $\boldsymbol{\varepsilon}_t$ given the information set $\mathcal{F}_{t-1}$ is a positive-definite $m \times m$ matrix.

It follows that the univariate representation of the conditional covariance and variance components are given by

$$\sigma_{ijt} = \rho_{ijt}(h_{it}g_{it})^{1/2}(h_{jt}g_{jt})^{1/2}, \quad i \neq j \tag{5}$$

and

$$\sigma_{iit} = h_{it}g_{it}, \quad i = 1, \ldots, m \tag{6}$$

respectively. In our approach we assume the variance process to be multiplicatively decomposed into a long-term component g_{it} introducing nonstationarity and describing the structural changes in the volatility clusters and a short-term component h_{it} describing conditional heteroskedasticity augmented with cross-asset (or cross-market) heteroskedastic effects. As in Amado and Teräsvirta (2014) the diagonal elements of $\mathbf{S}_t^2$ are defined as follows

$$g_{it} = g_{it}(\boldsymbol{\theta}_g, t/T) = \delta_{i0} + \sum_{j=1}^{r_i} \delta_{ij} G_{ij}(\gamma_{ij}, \mathbf{c}_{ij}; t/T), \tag{7}$$

where $\delta_{i0} > 0$ is a fixed (known) constant, $\delta_{ij} \neq 0$, $j = 1, \ldots, r_i$, and $\gamma_{ij} > 0$, $i = 1, \ldots, m$, $j = 1, \ldots, r_i$, and $r_i = 1, \ldots, R$, such that R is a finite integer. To prevent exchangeability of components in (7) further restrictions are needed on $\mathbf{c}_{ij}$. The function $G_{ij}(\gamma_{ij}, \mathbf{c}_{ij}; t/T)$ is the (generalised) logistic function

$$G_{ij}(\gamma_{ij}, \mathbf{c}_{ij}; t/T) = (1 + \exp\{-\gamma_{ij} \prod_{l=1}^{k_{ij}} (t/T - c_{ijl})\})^{-1} \tag{8}$$

where $\mathbf{c}_{ij} = (c_{ij1}, \ldots, c_{ijk_{ij}})'$ such that $c_{ij1} \leqslant c_{ij2} \leqslant \cdots \leqslant c_{ijk_{ij}}$. Function (8) is by construction continuous for $\gamma_{il} < \infty$, $i = 1, \ldots, m$, and bounded between zero and unity. The parameters c_{ilj} and γ_{il} determine the location and the speed of the transition between volatility regimes. Under $\delta_{i1} = ... = \delta_{ir_i} = 0$ or $\gamma_{i1} = ... = \gamma_{ir_i} = 0$, $i = 1, \ldots, m$, in (7), the unconditional variance of ε_t becomes constant, otherwise it is capable of describing smooth changes in the amplitude of volatility clusters. In the simplest case, $r_i = 1$ and $k_{ij} = 1$, the function g_{it} increases monotonically over time when $\delta_{i1} > 0$ and decreases monotonically when $\delta_{i1} < 0$. The slope parameter γ_{i1} in (8) controls the degree of smoothness of the transition function: the larger γ_{i1}, the faster the transition between the extreme states. As $\gamma_{i1} \longrightarrow \infty$, structural breaks can be identified at the location c_{i11}.

The diagonal components of $\mathbf{D}_t^2$ are assumed to follow a weakly stationary augmented GARCH(p, q) representation by rescaling the squared innovations with the deterministic function g_{it} and are defined as

$$h_{it} = h_{it}(\boldsymbol{\theta}_g, \boldsymbol{\theta}_h) = \omega_i + \sum_{k=1}^{q_i} \sum_{j=1}^{m} \alpha_{kij} \phi_{j,t-k}^2 + \sum_{k=1}^{p_i} \beta_{ki} h_{i,t-k}, \quad \omega_i > 0, \alpha_{kij} \geq 0, \beta_{ki} \geq 0, \quad (9)$$

where $\phi_{jt} = \varepsilon_{jt}/g_{jt}^{1/2}$, $j = 1, \ldots, m$. In this extension, the conditional variance of any element of $\boldsymbol{\phi}_t$ is allowed to depend on the past values of all elements.

For the correlation structure we employ the dynamic conditional correlation (DCC-)GARCH model by Engle (2002) where the conditional correlations depend upon the past standardized residuals as follows

$$q_{ij,t} = \bar{\rho}_{ij}(1 - a - b) + a z_{i,t-1} z_{j,t-1} + b q_{ij,t-1} \quad (10)$$

where a is a positive scalar and b is a non-negative scalar such that $a + b < 1$, $\bar{\rho}_{ij}$ is the unconditional correlation of the standardized innovations $z_{i,t}$ and $z_{j,t}$, and the correlation estimator

$$\rho_{ij,t} = \frac{q_{ij,t}}{\sqrt{q_{ii,t}}\sqrt{q_{jj,t}}} \quad (11)$$

ensures positive definiteness and produces valid correlation coefficients. The model defined in (1)–(11) shall be called the multiplicative time-varying extended dynamic conditional correlation (MTV-EDCC-)GARCH(p, q) model. A special case is nested in this model. When $\alpha_{kij} = 0$, $i \neq j$, $k = 1, \ldots, q_i$, the model excludes volatility interactions and the resulting model shall be called MTV-DCC-GARCH model. If we further let $\mathbf{S}_t \equiv \mathbf{I}_m$ the model collapses into the Dynamic Conditional Correlation (DCC-)GARCH(p, q) model of Engle (2002).

In the simplest form the conditional correlations are assumed to be time-invariant, i.e.,

$\mathbf{P}_t \equiv \mathbf{P}$ and this version of the model will be called the multiplicative time-varying extended constant conditional correlation (MTV-ECCC-)GARCH(p, q) model. If, additionally, $\mathbf{S}_t \equiv \mathbf{I}_m$, the model collapses into the ECCC-GARCH(p, q) model of Jeantheau (1998) and He and Teräsvirta (2004). The constant conditional correlation (CCC-)GARCH(p, q) model of Bollerslev (1990) is nested in the MTV-ECCC-GARCH(p, q) model when $\mathbf{P}_t \equiv \mathbf{P}$, $\mathbf{S}_t \equiv \mathbf{I}_m$ and $\alpha_{kij} = 0$, $i \neq j$, $k = 1, \ldots, q_i$,

3 Estimation of parameters

In this section, we are interested in estimating the conditional variance of each component of $\boldsymbol{\varepsilon}_t$ and the correlations of $\boldsymbol{\varepsilon}_t$ in $\mathbf{P}_t$. Since maximum likelihood estimation is numerically very difficult we shall apply maximization by parts by Song, Fan, and Kalbfleisch (2005) to the problem of maximizing the log-likelihood of the model. Firstly, the variance component is modelled according to the equation-by-equation strategy suggested by Francq and Zakoïan (2016) and then, secondly, the correlation component is obtained conditionally on the estimated variances.

We begin by introducing some notation. Let the vector of parameters be denoted by $\boldsymbol{\theta} = (\boldsymbol{\theta}'_\vartheta, \boldsymbol{\theta}'_\rho)'$ where the parameter vector $\boldsymbol{\theta}_\vartheta = (\boldsymbol{\theta}_g, \boldsymbol{\theta}_h)$ contains the parameters of the conditional variances and the elements of $\boldsymbol{\theta}_\rho$ are the parameters of the correlation matrix. The composition of $\boldsymbol{\theta}_\rho$ depends on the structure of the correlation matrix. Assuming $\boldsymbol{\varepsilon}_t|\mathcal{F}_{t-1} \sim \mathcal{N}(\mathbf{0}, \boldsymbol{\Sigma}_t)$, the conditional log-likelihood function for observation t of the model is defined as

$$\begin{aligned}
\ell_t(\boldsymbol{\theta}, \boldsymbol{\varepsilon}_t) &= -(m/2)\ln(2\pi) - (1/2)\ln|\boldsymbol{\Sigma}_t| - (1/2)\boldsymbol{\varepsilon}'_t\boldsymbol{\Sigma}_t^{-1}\boldsymbol{\varepsilon}_t \\
&= -(m/2)\ln(2\pi) - (1/2)\ln|\mathbf{S}_t\mathbf{D}_t\mathbf{P}_t\mathbf{D}_t\mathbf{S}_t| - (1/2)\boldsymbol{\varepsilon}'_t\mathbf{S}_t^{-1}\mathbf{D}_t^{-1}\mathbf{P}_t^{-1}\mathbf{D}_t^{-1}\mathbf{S}_t^{-1}\boldsymbol{\varepsilon}_t \\
&= -(m/2)\ln(2\pi) - \ln|\mathbf{S}_t\mathbf{D}_t| - (1/2)\ln|\mathbf{P}_t| - (1/2)\mathbf{z}'_t\mathbf{P}_t^{-1}\mathbf{z}_t \\
&= -(m/2)\ln(2\pi) - \ln|\mathbf{S}_t| - (1/2)\widetilde{\boldsymbol{\varepsilon}}'_t\mathbf{S}_t^{-2}\widetilde{\boldsymbol{\varepsilon}}_t - \ln|\mathbf{D}_t| - (1/2)\boldsymbol{\varepsilon}_t^{*\prime}\mathbf{D}_t^{-2}\boldsymbol{\varepsilon}_t^* \\
&\quad + \mathbf{z}'_t\mathbf{z}_t - (1/2)\ln|\mathbf{P}_t| - (1/2)\mathbf{z}'_t\mathbf{P}_t^{-1}\mathbf{z}_t \qquad (12)
\end{aligned}$$

where $\widetilde{\boldsymbol{\varepsilon}}_t = \mathbf{D}_t^{-1}\boldsymbol{\varepsilon}_t = (\varepsilon_{1t}/\{h_{1t}(\boldsymbol{\theta}_g, \boldsymbol{\theta}_h)\}^{1/2}, \ldots, \varepsilon_{mt}/\{h_{mt}(\boldsymbol{\theta}_g, \boldsymbol{\theta}_h)\}^{1/2})'$,

$\boldsymbol{\varepsilon}_t^* = \mathbf{S}_t^{-1}\boldsymbol{\varepsilon}_t = (\varepsilon_{1t}/\{g_{1t}(\boldsymbol{\theta}_g)\}^{1/2}, \ldots, \varepsilon_{mt}/\{g_{mt}(\boldsymbol{\theta}_g)\}^{1/2})'$ and

$\mathbf{z}_t = \mathbf{D}_t^{-1}\mathbf{S}_t^{-1}\boldsymbol{\varepsilon}_t = (\varepsilon_{1t}/\{h_{1t}(\boldsymbol{\theta}_g, \boldsymbol{\theta}_h)g_{1t}(\boldsymbol{\theta}_g)\}^{1/2}, \ldots, \varepsilon_{mt}/\{h_{mt}(\boldsymbol{\theta}_g, \boldsymbol{\theta}_h)g_{mt}(\boldsymbol{\theta}_g)\}^{1/2})'$.

Equation (12) implies the following decomposition of the log-likelihood function for observation t :

$$\ell_t(\boldsymbol{\theta}_\vartheta, \boldsymbol{\theta}_\rho) = \ell_t^U(\boldsymbol{\theta}_g) + \ell_t^V(\boldsymbol{\theta}_g, \boldsymbol{\theta}_h) + \ell_t^C(\boldsymbol{\theta}_g, \boldsymbol{\theta}_h, \boldsymbol{\theta}_\rho) \tag{13}$$

where $\ell_t^U(\boldsymbol{\theta}_g) = \sum_{i=1}^m \ell_{it}^U(\boldsymbol{\theta}_g)$ and $\ell_{it}^U(\boldsymbol{\theta}_g) = -(1/2)\{\ln g_{it}(\boldsymbol{\theta}_g) + \widetilde{\varepsilon}_{it}^2/g_{it}(\boldsymbol{\theta}_g)\}$. Furthermore, $\ell_t^V(\boldsymbol{\theta}_g, \boldsymbol{\theta}_h) = \sum_{i=1}^m \ell_{it}^V(\boldsymbol{\theta}_g, \boldsymbol{\theta}_h)$ and $\ell_{it}^V(\boldsymbol{\theta}_g, \boldsymbol{\theta}_h) = -(1/2)\{\ln h_{it}(\boldsymbol{\theta}_g, \boldsymbol{\theta}_h) + \varepsilon_{it}^{*2}/h_{it}(\boldsymbol{\theta}_g, \boldsymbol{\theta}_h)\}$. Finally,

$$\ell_t^C(\boldsymbol{\theta}_g, \boldsymbol{\theta}_h, \boldsymbol{\theta}_\rho) = -(1/2)\Big\{\ln|\mathbf{P}_t(\boldsymbol{\theta}_g, \boldsymbol{\theta}_h, \boldsymbol{\theta}_\rho)| - \mathbf{z}_t'\mathbf{P}_t^{-1}(\boldsymbol{\theta}_g, \boldsymbol{\theta}_h, \boldsymbol{\theta}_\rho)\mathbf{z}_t - 2\mathbf{z}_t'\mathbf{z}_t\Big\} \tag{14}$$

Similarly to the DCC-GARCH model, the model is naturally estimated with the two-step modelling strategy. First, the augmented GARCH equations are estimated using maximization by parts and thereafter the correlation matrix is estimated conditionally on the GARCH estimates. The iterative algorithm proceeds as follows.

Step 1: Maximize

$$L_{iT}^U(\boldsymbol{\theta}_g) = \sum_{t=1}^T \ell_{it}^U(\boldsymbol{\theta}_g) = -(1/2)\sum_{t=1}^T \{\ln g_{it}(\boldsymbol{\theta}_g) + \widetilde{\varepsilon}_{it}^2/g_{it}(\boldsymbol{\theta}_g)\} \tag{15}$$

with respect to $\boldsymbol{\theta}_g$ for each $i, i = 1, \ldots, m$, separately, assuming $\widetilde{\varepsilon}_{it}^* = \varepsilon_{it}$, that is, setting $h_{it}(\boldsymbol{\theta}_g, \boldsymbol{\theta}_h) \equiv 1$. Denote the estimator as $\widehat{\boldsymbol{\theta}}_g^{(1)}$. For identification reasons, the parameters δ_{0i} and γ_{0i} are fixed, respectively, to $\widehat{\delta}_{0i}$ and $\widehat{\gamma}_{0i}$. This means that the estimation algorithm is carried out without iterating δ_{0i} and γ_{0i}, $i = 1, , m$, and therefore the remaining parameters are estimated conditionally on those estimates. Making use of $\widehat{\boldsymbol{\theta}}_g^{(1)}$, maximize

$$L_{iT}^V(\widehat{\boldsymbol{\theta}}_g^{(1)}, \boldsymbol{\theta}_h) = \sum_{t=1}^T \ell_{it}^V(\widehat{\boldsymbol{\theta}}_g^{(1)}, \boldsymbol{\theta}_h) = -(1/2)\sum_{t=1}^T \{\ln h_{it}(\widehat{\boldsymbol{\theta}}_g^{(1)}, \boldsymbol{\theta}_h) + \boldsymbol{\varepsilon}_{it}^{*2}/h_{it}(\widehat{\boldsymbol{\theta}}_g^{(1)}, \boldsymbol{\theta}_h)\} \tag{16}$$

with respect to $\boldsymbol{\theta}_h$ for each $i, i = 1, \ldots, m$, where $\varepsilon_{it}^* = \varepsilon_{it}/\{g_{it}(\widehat{\boldsymbol{\theta}}_g^{(1)})\}^{1/2}$. Call the resulting estimator as $\widehat{\boldsymbol{\theta}}_h^{(1)}$.

Step 2: Maximize

$$L_{iT}^{U}(\boldsymbol{\theta}_g) = \sum_{t=1}^{T} \ell_{it}^{U}(\boldsymbol{\theta}_g) = -(1/2)\sum_{t=1}^{T}\{\ln g_{it}(\boldsymbol{\theta}_g) + \widetilde{\boldsymbol{\varepsilon}}_{it}^{2}/g_{it}(\boldsymbol{\theta}_g)\} \tag{17}$$

with respect to $\boldsymbol{\theta}_g$ where $\widetilde{\varepsilon}_{it} = \varepsilon_{it}/\{h_{it}(\widehat{\boldsymbol{\theta}}_g^{(1)}, \widehat{\boldsymbol{\theta}}_h^{(1)})\}^{1/2}$ for each $i, i = 1, \ldots, m$. Denote this estimator $\widehat{\boldsymbol{\theta}}_g^{(2)}$ and maximize

$$L_{iT}^{V}(\widehat{\boldsymbol{\theta}}_g^{(2)}, \boldsymbol{\theta}_h) = \sum_{t=1}^{T} \ell_{it}^{V}(\widehat{\boldsymbol{\theta}}_g^{(2)}, \boldsymbol{\theta}_h) = -(1/2)\sum_{t=1}^{T}\{\ln h_{it}(\widehat{\boldsymbol{\theta}}_g^{(2)}, \boldsymbol{\theta}_h) + \boldsymbol{\varepsilon}_{it}^{*2}/h_{it}(\widehat{\boldsymbol{\theta}}_g^{(2)}, \boldsymbol{\theta}_h)\} \tag{18}$$

with respect to $\boldsymbol{\theta}_h$, where $\varepsilon_{it}^{*} = \varepsilon_{it}/\{g_{it}(\widehat{\boldsymbol{\theta}}_g^{(2)})\}^{1/2}$. This yields the estimator $\widehat{\boldsymbol{\theta}}_h^{(2)}$. Iterate until convergence. Call the resulting estimators $\widehat{\boldsymbol{\theta}}_g$ and $\widehat{\boldsymbol{\theta}}_h$.

After estimating the variance equations, estimate $\boldsymbol{\theta}_\rho$ given $\widehat{\boldsymbol{\theta}}_g$ and $\widehat{\boldsymbol{\theta}}_h$ by maximizing

$$L_{iT}^{C}(\boldsymbol{\theta}_\rho) = \sum_{t=1}^{T} \ell_{t}^{C}(\boldsymbol{\theta}_\rho|\widehat{\boldsymbol{\theta}}_g, \widehat{\boldsymbol{\theta}}_h) = -(1/2)\Big\{\ln|\mathbf{P}_t(\boldsymbol{\theta}_\rho)| - \mathbf{z}_t'\mathbf{P}_t^{-1}(\boldsymbol{\theta}_\rho)\mathbf{z}_t - 2\mathbf{z}_t'\mathbf{z}_t\Big\} \tag{19}$$

where $\mathbf{z}_t = (z_{1t}, \ldots, z_{mt})$ with $z_{it} = \varepsilon_{it}/\{h_{it}(\widehat{\boldsymbol{\theta}}_g, \widehat{\boldsymbol{\theta}}_h)g_{it}(\widehat{\boldsymbol{\theta}}_g)\}^{1/2}$, $i = 1, \ldots, m$.

Under mild regularity conditions, Silvennoinen and Teräsvirta (2021) established consistency and asymptotic normality of the QMLE for the multivariate conditional correlation GARCH models with extended GARCH equations with a multiplicative deterministic component and time-varying correlations. Francq and Zakoïan (2016) showed strong consistency and asymptotic normality of the equation-by-equation estimator for fairly general conditional correlation GARCH models with variance interactions. Ling and McAleer (2003) also proved the asymptotic properties of the constant conditional correlation GARCH model without imposing any diagonality for the ARCH and GARCH matrices. However, in both cases, stationarity is imposed to the conditional variances. Extending their asymptotic results for the MTV-EDCC-GARCH model is a nontrivial problem and beyond the scope of the present paper. For inference, we shall assume that the asymptotic distribution of the equation-by-equation estimator is normal. It then follows that

$$\sqrt{T}(\widehat{\boldsymbol{\theta}}_T - \boldsymbol{\theta}_0) \xrightarrow{d} \mathcal{N}(\mathbf{0}, \mathcal{I}_T^{-1}(\boldsymbol{\theta}_0)). \tag{20}$$

where $\mathcal{I}_T(\boldsymbol{\theta}_0)$ is the population information matrix evaluated at the true parameter vector $\boldsymbol{\theta} = \boldsymbol{\theta}_0$.

4 Specific-to-general model selection

Our aim is to construct a coherent strategy for building MTV-ECC-GARCH models using statistical inference. The model-building cycle is similar to the specific-to-general strategy for nonlinear models of the conditional mean considered in, among others, Teräsvirta (1998) and Teräsvirta, Tjøstheim, and Granger (2010). This implies starting with a parsimonious model and proceeding to a more flexible variance model only if the statistical misspecification tests indicate that the maintained model is inadequate. The strategy for building MTV-ECC-GARCH models consists of specification, estimation and evaluation stages of the model. The technique involves a sequential procedure for specifying the parameterization of the deterministic component g_t and determining the shape of the transition function using a sequence of LM-type tests. In practice, the parametric structure of this volatility component has to be determined from the data, which involves finding the number of transitions r_i in (7) and selecting the integer k_{ij} in (8) with the testing procedure of Amado and Teräsvirta (2013). The modelling cycle for specifying the MTV-ECC-GARCH model consists of the following stages:

1. Begin by modelling the conditional variance h_{it} under the assumption that $g_{it} \equiv 1$ and $\alpha_{kij} \equiv 0$, $k = 1, \ldots, q_i, j = 1, \ldots, m, i \neq j$. This may be preceded by testing the null hypothesis of no ARCH using the Engle (1982) LM test. In case of rejection, a GARCH(1,1) model is estimated and tested against a MTV-GARCH model. The number of functions g_{it} is determined thereafter equation by equation by sequential testing. This is done as follows.

2. Test the hypothesis of constant unconditional variance $\mathrm{H}_{01}^{\textsf{TV-VOL}} : \gamma_{i1} = 0$ against $\mathrm{H}_{11}^{\textsf{TV-VOL}} : \gamma_{i1} > 0$ in

$$g_{it} = 1 + \delta_{i1} G_{i1}(\gamma_{i1}, \mathbf{c}_{i1}; t/T) \tag{21}$$

at the significance level $\alpha^{(1)}$. The standard test statistic has a non-standard asymptotic distribution because δ_{i1} and $\mathbf{c}_{i1}$ are unidentified nuisance parameters when $\mathrm{H}_{01}^{\textsf{TV-VOL}}$ is true. To circumvent this identification problem we follow Luukkonen, Saikkonen, and Teräsvirta (1988) and approximate $G_{i1}(\gamma_{i1}, \mathbf{c}_{i1}; t/T)$ by its third-order Taylor expansion around $\gamma_{i1} = 0$. After reparameterizing, we obtain

$$g_{it} = \omega_i^* + \sum_{j=1}^{3} \phi_{ij}(t/T)^j + R_3(\gamma_{i1}, \mathbf{c}_{i1}; t/T) \tag{22}$$

where $\phi_{ij} = \gamma_{i1}^j \widetilde{\delta}_{ij}^*$, with $\widetilde{\delta}_{ij}^* \neq 0$, and $R_3(\gamma_{i1}, \mathbf{c}_{i1}; t/T)$ is the remainder. Furthermore, $R_3(\gamma_{i1}, \mathbf{c}_{i1}; t/T) \equiv 0$ under $\mathrm{H}_{01}^{\textsf{TV-VOL}}$, so the remainder of the Taylor expansion does not affect the asymptotic distribution theory. The new null hypothesis based on this approximation becomes $\mathrm{H}_{01}^{\textsf{TV-VOL},*} : \phi_{i1} = \phi_{i2} = \phi_{i3} = 0$. Under $\mathrm{H}_{01}^{\textsf{TV-VOL},*}$, the standard LM statistic has an asymptotic χ^2-distribution with three degrees of freedom. See Amado and Teräsvirta (2017) for details on how to compute the test statistic. If $\mathrm{H}_{01}^{\textsf{TV-VOL},*}$ is rejected, for each equation select the order $k_{i1} \leq 3$ in the exponent of $G_{i1}(\gamma_{i1}, \mathbf{c}_{i1}; t/T)$ using a short sequence of tests within (22); for details see Amado and Teräsvirta (2017). In case of failure to reject the null hypothesis of constant unconditional variance estimate a standard GARCH model.

3. Next, if $\mathrm{H}_{01}^{\textsf{TV-VOL}}$ is rejected estimate g_{it} with a single transition function and test $\mathrm{H}_{02}^{\textsf{TV-VOL}} : \gamma_{i2} = 0$ against $\mathrm{H}_{12}^{\textsf{TV-VOL}} : \gamma_{i2} > 0$ in

$$g_{it} = 1 + \delta_{i1} G_{i1}(\gamma_{i1}, \mathbf{c}_{i1}; t/T) + \delta_{i2} G_{i2}(\gamma_{i2}, \mathbf{c}_{i2}; t/T) \tag{23}$$

at the significance level $\alpha^{(2)} = \tau\alpha^{(1)}$, where $\tau \in (0, 1)$. In our application we set $\tau = 0.5$. The significance level is reduced at each stage by a factor τ in order to favour parsimony. Again, model (23) is not identified under the null hypothesis. To circumvent the problem we proceed as before and express the logistic function $G_{i2}(\gamma_{i2}, \mathbf{c}_{i2}; t/T)$ by a third-order Taylor approximation around $\gamma_{i2} = 0$. After rearranging terms we have

$$g_{it} = \omega_i^* + \delta_{i1} G_1(\gamma_{i1}, \mathbf{c}_{i1}; t/T) + \sum_{j=1}^{3} \varphi_{ij}(t/T)^j + R_3(\gamma_{i2}, \mathbf{c}_{i2}; t/T) \tag{24}$$

where $\varphi_{ij} = \gamma_{i2}^{j}\widetilde{\delta}_{ij}^{*}$, $\widetilde{\delta}_{ij}^{*} \neq 0$ and $R_3(\gamma_{i2}, \mathbf{c}_{i2}; t/T)$ is the remainder. The new null hypothesis based on this approximation becomes $\mathrm{H}_{02}^{\textsf{TV-VOL},*} : \varphi_{i1} = \varphi_{i2} = \varphi_{i3} = 0$. Again, this hypothesis can be tested using a LM test. If the null hypothesis is rejected, specify k_{i2} for the second transition and estimate g_{it} with two transition functions.

4. More generally, when g_{it} has been estimated with $r_i - 1$ transition functions one tests for another transition in g_{it} using the significance level $\alpha^{(r_i)} = \tau\alpha^{(r_i-1)}$, $r_i = 2, 3, \ldots$. Testing for additional transitions in g_{it} continues until the first non-rejection of the null hypothesis. Proceed to the next step.

5. Next, test for the presence of causality in the variance (or volatility spillovers) by testing whether the off-diagonal elements of the ARCH matrix are equal to zero, that is, test $\mathrm{H}_{0i}^{\textsf{Causal-VOL}} : \alpha_{kij} = 0$, $k = 1, \ldots, q_i$, $j = 1, \ldots, m$ and $i \neq j$; a full description of this test is provided in Section 5. In case of rejection, the volatility h_{it} component is misspecified and therefore re-estimate the volatility model augmented with cross-asset (or cross-market) conditional heteroskedasticity. In case of failure to reject the null hypothesis of no variance interactions and constant unconditional variance tentatively accept the standard GARCH as a specification for h_{it}. If the model passes the statistical tests, tentatively accept it. Otherwise, re-specify the model equation by equation or consider another family of volatility models.

5 A test for causality in nonstationary variance

Understanding the transmission mechanism of financial shocks is crucial to identify the origins of shocks on asset (or market) returns. When volatility transmission occurs, the MTV-GARCH model is not yet sufficient to model the time dependence in the data as the conditional variance is explained only by past series information. Testing the presence of causality in variance (or cross-asset/cross-market conditional heteroskedasticity) with multiplicative decomposition is therefore an important statistical tool to validate the specification of the estimated model. In what follows we provide a brief description of the testing procedure based on the LM test principle.

In order to consider the testing problem assume that the null model is the MTV-GARCH model in which the GARCH component is, for notational convenience, of order one, i.e., $q_i = p_i = 1$ and $r_i = 1$. With this assumption the short-run dynamics of the variance becomes:

$$h_{it} = \omega_i + \sum_{j=1}^{m} \alpha_{ij}\phi_{j,t-1}^2 + \beta_i h_{i,t-1}, \quad \omega_i > 0, \alpha_{ij} \geq 0, j = 1, \ldots, m, \beta_i \geq 0. \tag{25}$$

Assuming $\boldsymbol{\theta}_{\vartheta i}$ the volatility parameter vector for equation i be partitioned into $\boldsymbol{\theta}_{\vartheta i} = (\boldsymbol{\theta}_g', \boldsymbol{\theta}_{hi}', \boldsymbol{\theta}_{fi}')'$, where $\boldsymbol{\theta}_g = (\boldsymbol{\theta}_{g1}, \ldots, \boldsymbol{\theta}_{gm})'$ with $\boldsymbol{\theta}_{gi} = (\delta_{i1}, \mathbf{c}_{i1}')'$[1] and $\mathbf{c}_{i1} = (c_{i11}, \ldots, c_{i1k_i})'$, $\boldsymbol{\theta}_{hi} = (\omega_i, \alpha_{ii}, \beta_i)'$ and $\boldsymbol{\theta}_{fi} = \{\alpha_{ij}\}$, $j = 1, \ldots, m$ and $i \neq j$, it is useful to define an augmented version of the MTV-GARCH model by assuming that the conditional variance component is additively misspecified as

$$\sigma_{it}^2 = \{h_{it}(\boldsymbol{\theta}_g, \boldsymbol{\theta}_{hi}) + f_{it}(\boldsymbol{\theta}_{fi})\} g_{it}(\boldsymbol{\theta}_g) \tag{26}$$

such that $f_{it}(\boldsymbol{\theta}_{fi}) = 0$ if and only if $\boldsymbol{\theta}_{fi} = \mathbf{0}_{m-1}$. In this setting, the null hypothesis of no causality in variance (or no volatility spillovers) equals $\boldsymbol{\theta}_{fi} = \mathbf{0}_{m-1}$. Equivalently, the null hypothesis equals $\alpha_{ij} = 0$, for all $j = 1, \ldots, m$ and $i \neq j$. The quasi-likelihood function for the volatility component for observation t, equation i, has the form

$$\ell_{it}(\boldsymbol{\theta}_{\vartheta i}) = -(1/2)\ln 2\pi - (1/2)\{\ln\{h_{it}(\boldsymbol{\theta}_g, \boldsymbol{\theta}_{hi}) + f_{it}(\boldsymbol{\theta}_{fi})\} + \ln g_{it}(\boldsymbol{\theta}_g)\} - \\ -(1/2)\boldsymbol{\varepsilon}_{it}^2/\{h_{it}(\boldsymbol{\theta}_g, \boldsymbol{\theta}_{hi}) + f_{it}(\boldsymbol{\theta}_{fi})\} g_{it}(\boldsymbol{\theta}_g)\} \tag{27}$$

To derive the LM test let $\mathbf{s}_t(\boldsymbol{\theta}_{\vartheta i}) = \partial \ell_{it}(\boldsymbol{\theta}_{\vartheta i})/\partial \boldsymbol{\theta}_{\vartheta i}$ be the score vector of (27) at each point in time where

$$\mathbf{s}_t(\boldsymbol{\theta}_{\vartheta i}) = (\frac{\partial \ell_{it}(\boldsymbol{\theta}_{\vartheta i})}{\partial \boldsymbol{\theta}_g'}, \frac{\partial \ell_{it}(\boldsymbol{\theta}_{\vartheta i})}{\partial \boldsymbol{\theta}_{hi}'}, \frac{\partial \ell_{it}(\boldsymbol{\theta}_{\vartheta i})}{\partial \boldsymbol{\theta}_{fi}'}) \tag{28}$$

[1]Note that parameters δ_{i0} and γ_{i1} are omitted since they are fixed from the first iteration.

is the form of the partitioned score vector, and let

$$\mathbf{s}(\boldsymbol{\theta}_{\vartheta i}) = (1/T)\sum_{t=1}^{T}\mathbf{s}_t(\boldsymbol{\theta}_{\vartheta i}) \tag{29}$$

be the average score where

$$\mathbf{s}(\boldsymbol{\theta}_{\vartheta i}) = (\mathbf{s}_g(\boldsymbol{\theta}_{\vartheta i})', \mathbf{s}_h(\boldsymbol{\theta}_{\vartheta i})', \mathbf{s}_f(\boldsymbol{\theta}_{\vartheta i})')' \tag{30}$$

with $\mathbf{s}_g(\boldsymbol{\theta}_{\vartheta i}) = (\mathbf{s}_{g1}(\boldsymbol{\theta}_{\vartheta i}), \ldots, \mathbf{s}_{gm}(\boldsymbol{\theta}_{\vartheta i}))'$. The components of (30) are

$$\mathbf{s}_{gi}(\boldsymbol{\theta}_{\vartheta i}) = (1/T)\sum_{t=1}^{T}\frac{\partial \ell_{it}(\boldsymbol{\theta}_{\vartheta i})}{\partial \boldsymbol{\theta}_{gi}} = (2T)^{-1}\sum_{t=1}^{T}(z_{it}^2-1)\left(\frac{1}{g_{it}}\frac{\partial g_{it}}{\partial \boldsymbol{\theta}_{gi}} + \frac{1}{f_{it}+h_{it}}\frac{\partial h_{it}}{\partial \boldsymbol{\theta}_{gi}}\right) \tag{31}$$

$$\mathbf{s}_{gj}(\boldsymbol{\theta}_{\vartheta i}) = (1/T)\sum_{t=1}^{T}\frac{\partial \ell_{it}(\boldsymbol{\theta}_{\vartheta i})}{\partial \boldsymbol{\theta}_{gj}} = (2T)^{-1}\sum_{t=1}^{T}(z_{it}^2-1)\frac{1}{f_{it}+h_{it}}\frac{\partial h_{it}}{\partial \boldsymbol{\theta}_{gj}} \tag{32}$$

$$\mathbf{s}_{h}(\boldsymbol{\theta}_{\vartheta i}) = (1/T)\sum_{t=1}^{T}\frac{\partial \ell_{it}(\boldsymbol{\theta}_{\vartheta i})}{\partial \boldsymbol{\theta}_{hi}} = (2T)^{-1}\sum_{t=1}^{T}(z_{it}^2-1)\frac{1}{f_{it}+h_{it}}\frac{\partial h_{it}}{\partial \boldsymbol{\theta}_{hi}} \tag{33}$$

$$\mathbf{s}_{f}(\boldsymbol{\theta}_{\vartheta i}) = (1/T)\sum_{t=1}^{T}\frac{\partial \ell_{it}(\boldsymbol{\theta}_{\vartheta i})}{\partial \boldsymbol{\theta}_{fi}} = (2T)^{-1}\sum_{t=1}^{T}(z_{it}^2-1)\frac{1}{f_{it}+h_{it}}\frac{\partial f_{it}}{\partial \boldsymbol{\theta}_{fi}} \tag{34}$$

for $j = 1, \ldots, m$, and $i \neq j$, where $z_{it} = \varepsilon_{it}/\{(f_{it}+h_{it})g_{it}\}^{1/2}$ and

$$\frac{\partial g_{it}}{\partial \boldsymbol{\theta}_{gi}} = (G_i(t/T), \mathbf{g}'_{c_i}(t/T))' \tag{35}$$

$$\frac{\partial h_{it}}{\partial \boldsymbol{\theta}_{gi}} = -\alpha_i\phi_{i,t-1}^2\frac{1}{g_{i,t-1}}\frac{\partial g_{i,t-1}}{\partial \boldsymbol{\theta}_{gi}} \tag{36}$$

$$\frac{\partial h_{it}}{\partial \boldsymbol{\theta}_{gj}} = -\alpha_{ij}\phi_{j,t-1}^2\frac{1}{g_{j,t-1}}\frac{\partial g_{j,t-1}}{\partial \boldsymbol{\theta}_{gj}} \tag{37}$$

$$\frac{\partial h_{it}}{\partial \boldsymbol{\theta}_{hi}} = \mathbf{v}_{i,t-1} + \beta_i\frac{\partial h_{i,t-1}}{\partial \boldsymbol{\theta}_{hi}} \tag{38}$$

$$\frac{\partial h_{it}}{\partial \boldsymbol{\theta}_{fi}} = \boldsymbol{\phi}_{-i,t-1}^2 + \beta_i\frac{\partial h_{i,t-1}}{\partial \boldsymbol{\theta}_{fi}} \tag{39}$$

with $\mathbf{v}_{it} = (1, \phi_{it}^2, h_{it})'$, $G_i(t/T) \equiv G_{i1}(\gamma_{i1}, \mathbf{c}_{i1}; t/T)$, $\mathbf{g}_{c_i}(t/T) = (g_{c_{i1}}(t/T), \ldots, g_{c_{ik_i}}(t/T))'$ with $g_{c_{ik}}(t/T) = \dfrac{\partial g_{it}(t/T)}{\partial c_{ik}} = -\gamma_{i1}\delta_{i1}G_i(t/T)(1-G_i(t/T))\prod_{l=1}^{k_i-1}(t/T-c_{il})$, $k, l = 1, \ldots, k_i$ and $l \neq k$ and $\boldsymbol{\phi}_{-i,t} = \{\phi_{jt}\}, j = 1, \ldots, m$ and $i \neq j$, and $\phi_{it} = \varepsilon_{it}/\sqrt{g_{it}}$. In other words, if $\boldsymbol{\phi}_t = (\phi_{1t}, \ldots, \phi_{mt})'$, $\boldsymbol{\phi}_{-i,t}$ contains all the elements but the ith element. Setting $\widehat{h}_{it} = h_{it}(\widehat{\boldsymbol{\theta}}_g, \widehat{\boldsymbol{\theta}}_{hi}, \mathbf{0})$ and $\widehat{g}_{it} = g_{it}(\widehat{\boldsymbol{\theta}}_g)$ and evaluating the average score under $\mathsf{H}_{0i} : \alpha_{ij} = 0$, for $j=1,\ldots,m$, and $i\neq j$, yields

$$\mathbf{s}_{gi}(\widehat{\boldsymbol{\theta}}_g,\widehat{\boldsymbol{\theta}}_{hi},\mathbf{0})=(2T)^{-1}\sum_{t=1}^{T}(\widehat{z}_{it}^2-1)\left(\frac{1}{\widehat{g}_{it}^0}\frac{\partial g_{it}}{\partial\boldsymbol{\theta}_{gi}}|_{\mathsf{H}_{0i}}+\frac{1}{\widehat{h}_{it}^0}\frac{\partial h_{it}}{\partial\boldsymbol{\theta}_{gi}}|_{\mathsf{H}_{0i}}\right) \tag{40}$$

$$\mathbf{s}_{gj}(\widehat{\boldsymbol{\theta}}_g,\widehat{\boldsymbol{\theta}}_{hi},\mathbf{0})=(2T)^{-1}\sum_{t=1}^{T}(\widehat{z}_{it}^2-1)\frac{1}{\widehat{h}_{it}^0}\frac{\partial h_{it}}{\partial\boldsymbol{\theta}_{gj}}|_{\mathsf{H}_{0i}} \tag{41}$$

$$\mathbf{s}_{h}(\widehat{\boldsymbol{\theta}}_g,\widehat{\boldsymbol{\theta}}_{hi},\mathbf{0})=(2T)^{-1}\sum_{t=1}^{T}(\widehat{z}_{it}^2-1)\frac{1}{\widehat{h}_{it}^0}\frac{\partial h_{it}}{\partial\boldsymbol{\theta}_{hi}}|_{\mathsf{H}_{0i}} \tag{42}$$

$$\mathbf{s}_{f}(\widehat{\boldsymbol{\theta}}_g,\widehat{\boldsymbol{\theta}}_{hi},\mathbf{0})=(2T)^{-1}\sum_{t=1}^{T}(\widehat{z}_{it}^2-1)\frac{1}{\widehat{h}_{it}^0}\frac{\partial h_{it}}{\partial\boldsymbol{\theta}_{fi}}|_{\mathsf{H}_{0i}} \tag{43}$$

where $\widehat{z}_{it}^2=\varepsilon_{it}^2/\widehat{h}_{it}^0\widehat{g}_{it}^0$ with $\widehat{h}_{it}^0$ and $\widehat{g}_{it}^0$ denoting, respectively, the conditional variance and the deterministic component estimated under H_{0i}. Under regularity conditions, Amado and Teräsvirta (2013) showed that the maximum likelihood estimators by maximization by parts lead to consistent and asymptotically normal estimates. It follows that $\widehat{\boldsymbol{\theta}}_g\longrightarrow\boldsymbol{\theta}_g^0$ and $\widehat{\boldsymbol{\theta}}_{hi}\longrightarrow\boldsymbol{\theta}_{hi}^0$ in probability as $T\longrightarrow\infty$, where $\boldsymbol{\theta}_g^0$ and $\boldsymbol{\theta}_{hi}^0$ are the true parameter vectors of $\widehat{\boldsymbol{\theta}}_g$ and $\widehat{\boldsymbol{\theta}}_{hi}$, respectively. Analogously, the partial derivatives (35)−(39), evaluated at H_{0i}, simplify to

$$\frac{\partial g_{it}}{\partial\boldsymbol{\theta}_{gi}}|_{\mathsf{H}_{0i}}=(\widehat{G}_{it},\widehat{\mathbf{g}}_{c_i}'(t/T))' \tag{44}$$

$$\frac{\partial h_{it}}{\partial\boldsymbol{\theta}_{gi}}|_{\mathsf{H}_{0i}}=-\widehat{\alpha}_i\widehat{\phi}_{i,t-1}^2\frac{1}{\widehat{g}_{i,t-1}^0}\frac{\partial g_{i,t-1}}{\partial\boldsymbol{\theta}_{gi}}|_{\mathsf{H}_{0i}} \tag{45}$$

$$\frac{\partial h_{it}}{\partial\boldsymbol{\theta}_{gj}}|_{\mathsf{H}_{0i}}=0$$

$$\frac{\partial h_{it}}{\partial\boldsymbol{\theta}_{hi}}|_{\mathsf{H}_{0i}}=\widehat{\mathbf{v}}_{i,t-1}+\widehat{\beta}_i\frac{\partial h_{i,t-1}}{\partial\boldsymbol{\theta}_{hi}}|_{\mathsf{H}_{0i}} \tag{46}$$

$$\frac{\partial h_{it}}{\partial\boldsymbol{\theta}_{fi}}|_{\mathsf{H}_{0i}}=\widehat{\boldsymbol{\phi}}_{-i,t-1}^2+\widehat{\beta}_i\frac{\partial\widehat{h}_{i,t-1}}{\partial\boldsymbol{\theta}_{fi}}|_{\mathsf{H}_{0i}} \tag{47}$$

where $\widehat{\mathbf{v}}_{it}=(1,\widehat{\phi}_{it}^2,\widehat{h}_{it}^0)'$, $\widehat{G}_i(t/T)\equiv\widehat{G}_{i1}(\widehat{\gamma}_{i1},\widehat{\mathbf{c}}_{i1};t/T)$, $\widehat{\mathbf{g}}_{c_i}(t/T)=(\widehat{g}_{c_{i1}}(t/T),\ldots,\widehat{g}_{c_{ik_i}}(t/T))'$ with $\widehat{g}_{c_{ik}}(t/T)=\dfrac{\partial\widehat{g}_{it}(t/T)}{\partial c_{ik}}=-\widehat{\gamma}_{i1}\widehat{\delta}_{i1}\widehat{G}_i(t/T)(1-\widehat{G}_i(t/T))\prod_{l=1}^{k_i-1}(t/T-\widehat{c}_{il})$, $k,l=1,\ldots,k_i$ and $l\neq k$ and $\widehat{\boldsymbol{\phi}}_{-i,t}=\widehat{\phi}_{jt}$, $j=1,\ldots,m$, $i\neq j$, and $\widehat{\phi}_{it}=\varepsilon_{it}/\sqrt{\widehat{g}_{it}^0}$.

Let $\widehat{\boldsymbol{\theta}}_{\vartheta i}=(\widehat{\boldsymbol{\theta}}_g',\widehat{\boldsymbol{\theta}}_{hi}',\widehat{\boldsymbol{\theta}}_{fi}')'$ be the quasi-maximum likelihood estimator of $\boldsymbol{\theta}_{\vartheta i}$. The average score evaluated at $\widehat{\boldsymbol{\theta}}_{\vartheta i}$ under the null hypothesis equals

$$\mathbf{s}(\widehat{\boldsymbol{\theta}}_{\vartheta i}) = (\mathbf{s}_g(\widehat{\boldsymbol{\theta}}_{\vartheta i})', \mathbf{s}_h(\widehat{\boldsymbol{\theta}}_{\vartheta i})', \mathbf{s}_f(\widehat{\boldsymbol{\theta}}_{\vartheta i})')' = (\mathbf{0}', \mathbf{0}', \mathbf{s}_f(\widehat{\boldsymbol{\theta}}_g, \widehat{\boldsymbol{\theta}}_{hi}, \mathbf{0})')' \tag{48}$$

where $\mathbf{s}_f(\widehat{\boldsymbol{\theta}}_g, \widehat{\boldsymbol{\theta}}_{hi}, \mathbf{0})$ given in (43) is the relevant (nonzero) block in the LM test statistic.

Denoting the population information matrix by

$$\mathcal{I}_i(\boldsymbol{\theta}^0_{\vartheta i}) = \mathsf{E}\mathbf{s}(\boldsymbol{\theta}^0_{\vartheta i})\mathbf{s}(\boldsymbol{\theta}^0_{\vartheta i})' = \begin{bmatrix} \mathcal{I}_{hh,i}(\boldsymbol{\theta}^0_{\vartheta i}) & \mathcal{I}_{hg,i}(\boldsymbol{\theta}^0_{\vartheta i}) & \mathcal{I}_{hf,i}(\boldsymbol{\theta}^0_{\vartheta i}) \\ \mathcal{I}_{gh,i}(\boldsymbol{\theta}^0_{\vartheta i}) & \mathcal{I}_{gg,i}(\boldsymbol{\theta}^0_{\vartheta i}) & \mathcal{I}_{gf,i}(\boldsymbol{\theta}^0_{\vartheta i}) \\ \mathcal{I}_{fh,i}(\boldsymbol{\theta}^0_{\vartheta i}) & \mathcal{I}_{fg,i}(\boldsymbol{\theta}^0_{\vartheta i}) & \mathcal{I}_{ff,i}(\boldsymbol{\theta}^0_{\vartheta i}) \end{bmatrix} \tag{49}$$

where $\boldsymbol{\theta}^0_{\vartheta i}$ is the true volatility parameter vector and $\mathbf{s}(\boldsymbol{\theta}^0_{\vartheta i})$ is $\mathbf{s}(\boldsymbol{\theta}_{\vartheta i})$ evaluated at $\boldsymbol{\theta}^0_{\vartheta i}$, the corresponding south-east block of the inverse of $\mathcal{I}_i(\boldsymbol{\theta}^0_{\vartheta i})$ evaluated under the H_{0i} equals

$$\mathcal{I}^{-1}_{ff}(\widehat{\boldsymbol{\theta}}_{\vartheta i}) = \{\mathcal{I}_{ff}(\widehat{\boldsymbol{\theta}}_{\vartheta i}) - \mathcal{I}_{f\cdot}(\widehat{\boldsymbol{\theta}}_{\vartheta i})[\mathcal{I}_{\cdot\cdot}(\widehat{\boldsymbol{\theta}}_{\vartheta i})]^{-1}\mathcal{I}_{\cdot f}(\widehat{\boldsymbol{\theta}}_{\vartheta i})\}^{-1} \tag{50}$$

where

$$\mathcal{I}_{\cdot\cdot}(\widehat{\boldsymbol{\theta}}_{\vartheta i}) = \begin{bmatrix} \hat{\mathcal{I}}_{hh,i}(\widehat{\boldsymbol{\theta}}_{\vartheta i}) & \hat{\mathcal{I}}_{hg,i}(\widehat{\boldsymbol{\theta}}_{\vartheta i}) \\ \hat{\mathcal{I}}_{gh,i}(\widehat{\boldsymbol{\theta}}_{\vartheta i}) & \hat{\mathcal{I}}_{gg,i}(\widehat{\boldsymbol{\theta}}_{\vartheta i}) \end{bmatrix} \tag{51}$$

and

$$\mathcal{I}_{f\cdot}(\widehat{\boldsymbol{\theta}}_{\vartheta i}) = \begin{bmatrix} \mathcal{I}_{fh,i}(\widehat{\boldsymbol{\theta}}_{\vartheta i}) & \mathcal{I}_{fg,i}(\widehat{\boldsymbol{\theta}}_{\vartheta i}) \end{bmatrix} = \mathcal{I}'_{\cdot f}(\widehat{\boldsymbol{\theta}}_{\vartheta i}) \tag{52}$$

such that $\mathcal{I}_i(\boldsymbol{\theta}^0_{\vartheta i})$ can be consistently estimated by

$$\mathcal{I}_i(\widehat{\boldsymbol{\theta}}_{\vartheta i}) = T^{-1}\sum_{t=1}^{T}\mathbf{s}_t(\widehat{\boldsymbol{\theta}}_{\vartheta i})\mathbf{s}_t(\widehat{\boldsymbol{\theta}}_{\vartheta i})' \tag{53}$$

as shown by Ling and McAleer (2003). We now state our main result. Theorem 1 presents the univariate LM statistic for the misspecification test of no causality in variance.

Theorem 1 (Univariate test statistic). *Consider the multiplicative variance decomposition* $\sigma_{iit} = h_{it}g_{it}$ *whose components are defined in (7)-(9). Under* $\mathsf{H}_{0i} : \boldsymbol{\theta}_{fi} = \mathbf{0}_{m-1}$*, the*

LM statistic

$$LM_i = T\mathbf{s}_f'(\widehat{\boldsymbol{\theta}}_{\vartheta i})\mathcal{I}_{ff}^{-1}(\widehat{\boldsymbol{\theta}}_{\vartheta i})\mathbf{s}_f'(\widehat{\boldsymbol{\theta}}_{\vartheta i}) \tag{54}$$

where $\widehat{\boldsymbol{\theta}}_{\vartheta i}$ *is a consistent estimator of* $\boldsymbol{\theta}_{\vartheta i}^0$ *under* H_{0i}*, is asymptotically* χ^2*-distributed with* $m-1$ *degrees of freedom.*

In practice, an asymptotically equivalent test to the LM test in Theorem 1 may be carried out in a straightforward way using an auxiliary least squares regression as follows:

1. Estimate consistently the MTV-GARCH model by maximization by parts, save the standardized residuals $\widehat{z}_{it}^2 = \varepsilon_{it}^2/\widehat{h}_{it}^0\widehat{g}_{it}^0$, and compute the "residual sum of squares" $SSR_{0i} = \sum_{t=1}^T(\widehat{z}_{it}^2 - 1)^2$.

2. Regress $\widehat{z}_{it}^2 - 1$ on $\widehat{\mathbf{x}}_{it}^{hh} = \widehat{h}_{it}^{-1}\partial h_{it}/\partial\boldsymbol{\theta}_{hi}|_{\mathsf{H}_{0i}}$, $\widehat{\mathbf{x}}_{it}^{hg} + \widehat{\mathbf{x}}_{it}^{gg} = \widehat{h}_{it}^{-1}\partial h_{it}/\partial\boldsymbol{\theta}_{gi}|_{\mathsf{H}_{0i}} + \widehat{g}_{it}^{-1}\partial g_{it}/\partial\boldsymbol{\theta}_{gi}|_{\mathsf{H}_{0i}}$ and $\widehat{\mathbf{x}}_{it}^{hf} = \widehat{h}_{it}^{-1}\partial h_{it}/\partial\boldsymbol{\theta}_{fi}|_{\mathsf{H}_{0i}}$, and obtain the residual sum of squares SSR_{1i}.

3. Compute the test statistic

$$\xi_{LMnr,i} = T\frac{SSR_{0i} - SSR_{1i}}{SSR_{0i}} \tag{55}$$

   which has an asymptotic χ^2 distribution with $m-1$ degrees of freedom under the null hypothesis.

To further examine whether the coefficients of the additive component in the augmented version of equation (26) for each $i = 1, \ldots, m$, are jointly zero, we propose a multivariate version of the LM-type test statistic (54)-(55). The extension of the univariate case to the multivariate case is straightforward and the multivariate test statistic is presented in Corollary 1.1.

Corollary 1.1 (Multivariate test statistic). *Consider the multiplicative variance decomposition* $\sigma_{iit} = h_{it}g_{it}$ *whose components are defined in (7)-(9). Due to the block-diagonality of the information matrix, under the null hypothesis* $\mathsf{H}_0 : \boldsymbol{\theta}_{\vartheta f} = (\boldsymbol{\theta}_{\vartheta f1}', \ldots, \boldsymbol{\theta}_{\vartheta fm}')' = \mathbf{0}_{m(m-1)}$*, the multivariate LM statistic defined by*

$$\xi_{LMnr} = \sum_{i=1}^m \xi_{LMnr,i} \tag{56}$$

where $\xi_{LMnr,i}$ *is given by (55) for each* $i = 1, \ldots, m$*, has an asymptotic* χ^2 *distribution with* $\dim(\boldsymbol{\theta}_{\vartheta f})$ *degrees of freedom.*

The robust versions of the univariate and multivariate test statistics against nonnormal innovations can be constructed using Procedure 4.1 in Wooldridge (1990). The robust univariate test statistic can be computed as follows:

1. Estimate consistently the MTV-GARCH model by maximization by parts and save the standardized residuals $\widehat{z}_{it}^2 = \varepsilon_{it}^2 / \widehat{h}_{it}^0 \widehat{g}_{it}^0$.
2. Regress $\widehat{\mathbf{x}}_{it}^{hf}$ on $\widehat{\mathbf{x}}_{it}^{hh}$ and $\widehat{\mathbf{x}}_{it}^{hg} + \widehat{\mathbf{x}}_{it}^{gg}$, and save the vector of residuals $\widehat{\mathbf{r}}_{it}$.
3. Regress $\mathbf{1}_T$ on $(\widehat{z}_{it}^2 - 1)\widehat{\mathbf{r}}_{it}$ and compute the sum of squared residuals SSR_i.
4. Compute the robust test statistic

$$\xi_{LMr,i} = T - SSR_i \tag{57}$$

   which, under H_{0i}, is asymptotically χ^2-distributed with $m - 1$ degrees of freedom.

Analogously to the nonrobust case, to obtain the robust multivariate test statistic, repeat steps 1–4 and compute the χ^2-distributed statistic with $m(m-1)$ degrees of freedom as

$$\xi_{LMr} = \sum_{i=1}^{m} \xi_{LMr,i}, \tag{58}$$

under the null hypothesis.

6 Monte Carlo experiment

In this section we study the finite sample properties of the test proposed in Section 5. This is done by conducting a Monte Carlo experiment to study the empirical size and the power of the test statistics. These properties are investigated for bivariate series at different sample sizes $T = 1000, 2500$ and 5000 observations. We generated 5000 replications for each data generating process (DGP) and discarded the first 1000 observations to avoid any initialization effects.

The volatility component of the bivariate series is generated according to the multiplicative specification (1)−(9) assuming normal errors with $p = q = 1$ and $m = 2$. Under H_{0i} there is no causation in the second moment and the conditional variance component is described by the MTV-GARCH model as in Amado and Teräsvirta (2013). Under the alternative, causation in the conditional variance is introduced by letting $\alpha_{ij} \neq 0$, for all $j = 1, \ldots, m$ and $i \neq j$ to be non-negative. For the empirical size of the LM-type statistic we generated bivariate series from the first-order MTV-CCC-GARCH model. For the correlation component, we consider constant conditional correlations between the two series in the model which varies throughout from moderate correlation ($\rho = 0.5$) to high correlation ($\rho = 0.85$.) The size simulations are carried out for four different MTV-CCC-GARCH DGPs whose parameter values can be found in Table 1. These DGPs are intended to have different levels of persistence in volatility that goes from moderate persistence to high persistence ($\alpha_i + \beta_i = 0.95, 0.90$, $i = 1, 2$, in DGP3) and very high persistence ($\alpha_i + \beta_i = 0.95, 0.99$, $i = 1, 2$, in DGP1, DGP2 and DGP4). Finally, DGP2 and DGP4 are characterized by larger fluctuations in the long-term volatilities compared to DGP1 and DGP3. The parameter values are chosen such that they resemble results often found in fitting MTV-GARCH models to financial return series.

Results of the size simulations are presented graphically in Figure 1. The graphs show for the univariate and multivariate test statistics the discrepancies in size (the actual size minus the nominal size) against the nominal significance levels ranging from 0.1% to 10%. Only the results of the robust test statistics are reported given their superiority compared to the nonrobust test statistics. In each subgraph we present the size discrepancies of the robust univariate and multivariate test statistics for DGP1 − DGP4 and each sample size. One can visualize that the size distortions are, in general, small, decreasing with the number of observations and increasing with the correlation. The difference between the empirical rejection frequency and the nominal level appears to be larger for higher time dependence in volatility. Results from additional simulated models, not reported for the sake of saving space, further support this conclusion. There is also evidence that the univariate robust test statistics outperform the multivariate robust ones for the sample sizes considered.

Table 1: DGPs for the bivariate first-order MTV-CCC-GARCH model for size simulations. The total number of replications equals 5000.

	Stationary component	*Nonstationary component*	*Correlation*
DGP1	$h_{1t} = 0.10 + 0.10\phi^2_{1,t-1} + 0.85h_{1,t-1}$ $h_{2t} = 0.20 + 0.05\phi^2_{2,t-1} + 0.94h_{2,t-1}$	$g_{1t} = 1.2 - 0.05G_{1t}(5, 0.25; t/T)$ $g_{2t} = 1.2 + 0.05G_{2t}(10, 0.50; t/T)$	$\rho_{12} = 0.50$
DGP2	$h_{1t} = 0.10 + 0.10\phi^2_{1,t-1} + 0.85h_{1,t-1}$ $h_{2t} = 0.20 + 0.05\phi^2_{2,t-1} + 0.94h_{2,t-1}$	$g_{1t} = 1.0 - 0.05G_{1t}(5, 0.25; t/T)$ $g_{2t} = 2.5 + 0.05G_{2t}(10, 0.50; t/T)$	$\rho_{12} = 0.50$
DGP3	$h_{1t} = 0.10 + 0.10\phi^2_{1,t-1} + 0.85h_{1,t-1}$ $h_{2t} = 0.20 + 0.05\phi^2_{2,t-1} + 0.85h_{2,t-1}$	$g_{1t} = 1.2 - 0.05G_{1t}(5, 0.25; t/T)$ $g_{2t} = 1.2 + 0.05G_{2t}(10, 0.50; t/T)$	$\rho_{12} = 0.85$
DGP4	$h_{1t} = 0.10 + 0.10\phi^2_{1,t-1} + 0.85h_{1,t-1}$ $h_{2t} = 0.20 + 0.05\phi^2_{2,t-1} + 0.94h_{2,t-1}$	$g_{1t} = 1.2 - 0.75G_{1t}(5, 0.25; t/T)$ $g_{2t} = 1.2 + 1.50G_{2t}(10, 0.50; t/T)$	$\rho_{12} = 0.50$

Next we examine the power properties of the univariate and multivariate test statistics in finite sample. In order to discuss the performance of the testing procedure when the true model allows for causality in the conditional variance we generate a bivariate MTV-ECCC-GARCH model. The selected structures of the stationary and nonstationary components of the conditional variance and the correlation are summarized in Table 2. In what follows, we only report results of the power simulations for the robust version of the test statistics. Since the robust tests have good size properties we simply report the power curves instead of the size-adjusted rejection rates. As before we consider sample sizes of 1000, 2500 and 5000 observations and for every sample size and each DGP, 5000 Monte Carlo replications are carried out. The causality in the conditional variance ranges from a low level in time series 1 ($\alpha_{12} = 0.006$) to moderate level in time series 2 ($\alpha_{21} = 0.05$) for DGP5. The remaining DGPs generates realizations with moderate levels of causality in the conditional variance ($\alpha_{12} = \alpha_{21} = 0.05$). Volatility persistence ranges from moderate in DGP6-DGP7 to high in DGP8 and very high in DGP5. Correlation coefficients can be moderate as in DGP5$-$DGP6 ($\rho_{12} = 0.50$), very high as in DGP 7 ($\rho_{12} = 0.90$) or low as in DGP8 ($\rho_{12} = 0.30$). The power curves are depicted in Figure 2. On each graph, the actual rejection frequencies are plotted against the nominal significance levels 0.1%,0.2%,. . . ,10%. As expected, the power of the tests is an increasing function of the number of observations and levels of causality in the conditional variance (the power is relatively higher for series 2 in DGP5). The power seems to decrease when persistence in volatility is higher (as in

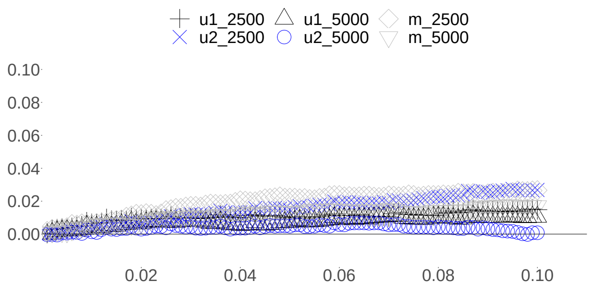

(a) DGP1

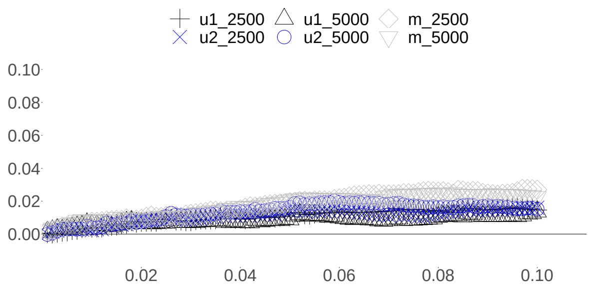

(b) DGP2

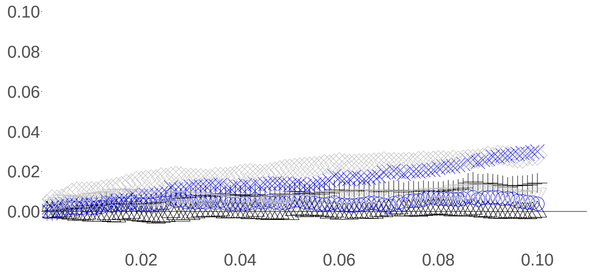

(c) DGP3

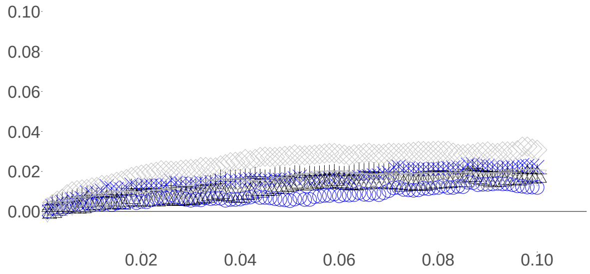

(d) DGP4

Figure 1: Size discrepancies plots of the causality-in-variance test for the bidimensional case. The size discrepancies of the robust LM tests are plotted against the nominal size. Results are shown for the univariate robust (ui_T) and multivariate robust (m_T) test statistics defined, respectively, in (57) and (58), $i = 1, 2$, for $T = 2500, 5000$.

DGP5 and DGP8) or when correlation is very high (as in DGP7).

7 Application: Causality in the volatility of carbon markets

In this section, we shall consider an empirical example to illustrate the application of the proposed model in Section 2 to real data. Our model is applied to daily returns of carbon emissions futures and media-based climate concerns index[2].

Carbon markets are the systems in which carbon credits are traded. To compensate for

[2]We also apply the test for causality in variance and the modelling strategy to exchange rate data. The data employed are daily returns of four major spot exchange rates against the euro, among the most traded currencies, from the Bank of England Database. The observation period starts in January 5, 1999 and ends in September 17, 2010, yielding a total of 2998 observations. Francq and Zakoïan (2012) studied the volatility comovements of the bivariate returns of the daily U.S. dollar and the Japanese yen exchange rates for the exact same period and three subperiods. Their results indicate that the volatility parameters appear to suffer from structural changes from one subperiod to another. The evidence of nonstationarity suggests that their constant conditional correlation asymmetric GARCH model may not be the most appropriate for fitting the data. Results are available in the supplementary material.

Table 2: DGPs for the bivariate first-order MTV-ECCC-GARCH model for power simulations. The total number of replications equals 5000.

	Stationary component	*Nonstationary component*
DGP5	$h_{1t} = 0.10 + 0.05\phi^2_{1,t-1} + 0.006\phi^2_{2,t-1} + 0.85h_{1,t-1}$	$g_{1t} = 1.50 - 0.05G_{1t}(5, 0.25)$
	$h_{2t} = 0.10 + 0.05\phi^2_{1,t-1} + 0.05\phi^2_{2,t-1} + 0.85h_{2,t-1}$	$g_{2t} = 1.00 + 0.10G_{2t}(10, 0.50)$
DGP6	$h_{1t} = 0.05 + 0.05\phi^2_{1,t-1} + 0.05\phi^2_{2,t-1} + 0.80h_{1,t-1}$	$g_{1t} = 0.95 + 0.05G_{1t}(5, 0.50)$
	$h_{2t} = 0.05 + 0.05\phi^2_{1,t-1} + 0.05\phi^2_{2,t-1} + 0.80h_{2,t-1}$	$g_{2t} = 1.05 - 0.03G_{2t}(5, 0.50)$
DGP7	$h_{1t} = 0.05 + 0.05\phi^2_{1,t-1} + 0.05\phi^2_{2,t-1} + 0.80h_{1,t-1}$	$g_{1t} = 0.95 + 0.05G_{1t}(5, 0.50)$
	$h_{2t} = 0.05 + 0.05\phi^2_{1,t-1} + 0.05\phi^2_{2,t-1} + 0.80h_{2,t-1}$	$g_{2t} = 1.05 - 0.03G_{2t}(5, 0.50)$
DGP8	$h_{1t} = 0.05 + 0.05\phi^2_{1,t-1} + 0.05\phi^2_{2,t-1} + 0.85h_{1,t-1}$	$g_{1t} = 0.95 + 0.05G_{1t}(5, 0.50)$
	$h_{2t} = 0.05 + 0.05\phi^2_{1,t-1} + 0.05\phi^2_{2,t-1} + 0.85h_{2,t-1}$	$g_{2t} = 1.05 - 0.03G_{2t}(5, 0.50)$

Correlation
DGP5: $\rho = 0.50$, DGP6: $\rho = 0.50$, DGP7: $\rho = 0.90$, DGP8: $\rho = 0.30$

their greenhouse gas (GHG) emissions, larger emitting entities can purchase carbon credits from those that remove or reduce emissions. One tradable carbon credit corresponds to one tonne of carbon dioxide (CO2) or the equivalent amount of a different GHG reduced, sequestered or avoided. When such credit is used, it becomes an offset and can no longer be traded. There are two main types of carbon markets. Compliance markets are established to adhere to regional, national, and/or international policy or regulatory mandates. Voluntary carbon markets, both at the national and international levels, involve the issuance, purchase, and sale of carbon credits on a voluntary basis. The European Union (EU) emissions trading system (ETS) is the carbon compliance market where EU emissions allowances, representing the right to emit one tonne of CO2 equivalent, are traded. Operating since 2005, it constitutes a cornerstone of the EUs climate policy and a key tool for cutting GHG emissions in the EU. Implemented in different phases, whose scope has been limited in terms of sector coverage but increasingly ambitious, in 2021 which marked the start of Phase 4, it covered around 40% of the EUs GHG emissions. Carbon futures contracts are standardized agreements that allow participants in the EU ETS to buy or sell allowances for a specific future trading period. These contracts specify the quantity of allowances, the price per allowance, the delivery date and can be used for different purposes such as hedging and speculation. For instance, companies with emission reduction targets

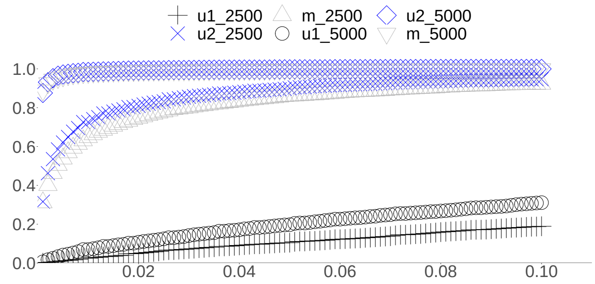

(a) DGP5

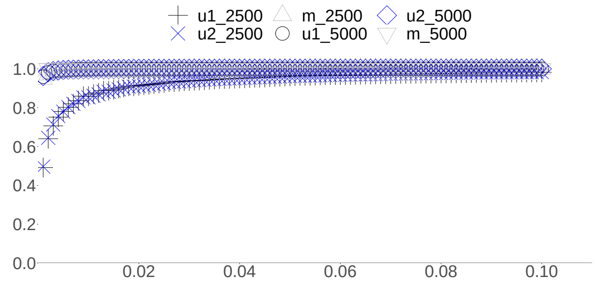

(b) DGP6

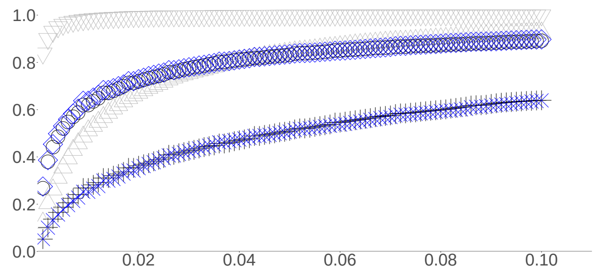

(c) DGP7

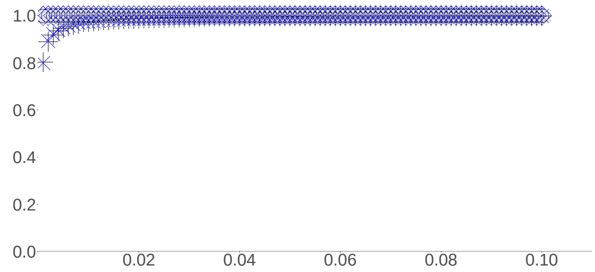

(d) DGP8

Figure 2: Power curves of the causality-in-variance test for the bidimensional case. The actual rejection frequency is plotted against the nominal size. Results are shown for the univariate robust (ui_T) and multivariate robust (m_T) test statistics defined, respectively, in (57) and (58), $i = 1, 2$, for $T = 2500, 5000$.

may use carbon futures to hedge against price volatility and secure future allowances at a known cost. Traders and speculators can also participate in the market to profit from price fluctuations. The price of carbon futures is influenced by various factors, including the overall demand for allowances, the regulatory environment, the economic conditions, and the success of emissions reduction efforts by participating entities. At the end of the futures contracts specified period, the actual emissions data is compared to the number of allowances surrendered by the participants. If a company has emitted less than its allocated allowances, it can sell its surplus. Conversely, companies that have emitted more than their allocated allowances must buy additional to cover the excess emissions. In this work we use the daily price of carbon emissions futures (CEF) expiring in December 2023. Surplus allowances can be purchased to cover future needs, creating a strong link between spot and futures prices. The cost of storing allowances is small and the main difference between a spot and a future emissions allowance is the opportunity cost of money paid for the spot allowance (https://www.ecb.europa.eu/pub/economic-bulletin/focus/2021/html/ecb.ebbox202106_05~ef8ce0bc70.en.html). The data covers the period starting on April 25th, 2005 until July 6th, 2023. A graph of the series is depicted in Figure 3.

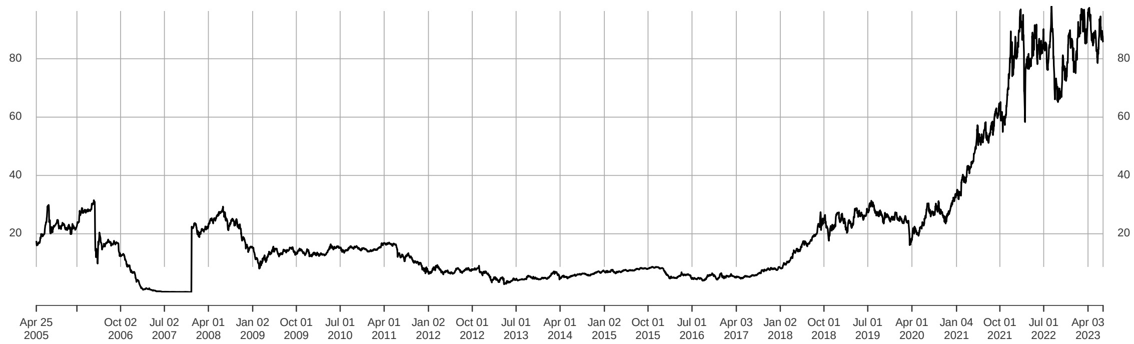

Figure 3: The daily price of carbon emissions futures.

The first phase of the EU ETS spanned the years 2005-2007 and was characterized by relatively unstable futures prices, collapsing to zero at the end of the phase, and oversupply of allowances. The second phase, which occurred between 2008 and 2012, coincided with the global financial crisis whose consequent reduced economic activity and emissions resulted in a demand-supply imbalance. Albeit volatile during the crisis, futures prices remained relatively low and stable for the rest of this period. The same effect is visible in the first years of Phase 3, which started in 2013 and ended in 2020. The third phase marked a progressive shift from free allowances, which were then attributed based on decarbonisation efforts, toward auctions, the introduction of mechanisms to correct for demand-supply imbalances and a reduction path for the EU-wide cap. Phase 3 was also characterized by a steep increase in futures prices which started rising in around 2018. The last phase, which started in 2021 and will last until 2030, is the most ambitious so far. Since then, there have been no signs of stabilising futures prices which progressively continued increasing and volatile. For this phase, the annual reduction path for the cap is planned to be increased and the stabilising mechanisms strengthened. More stringent climate policies and a possibly earlier end to the free allocation of emissions allowances are amongst the drivers of this price increase. The daily price series is then transformed into continuously compounded rates of return and multiplied by 100%. Figure 4 shows the daily log-returns on the carbon emissions futures.

To avoid convergence issues in the estimation, we truncate extreme returns (100%) to a maximum absolute value of 50%. We observe periods of increased volatility, where

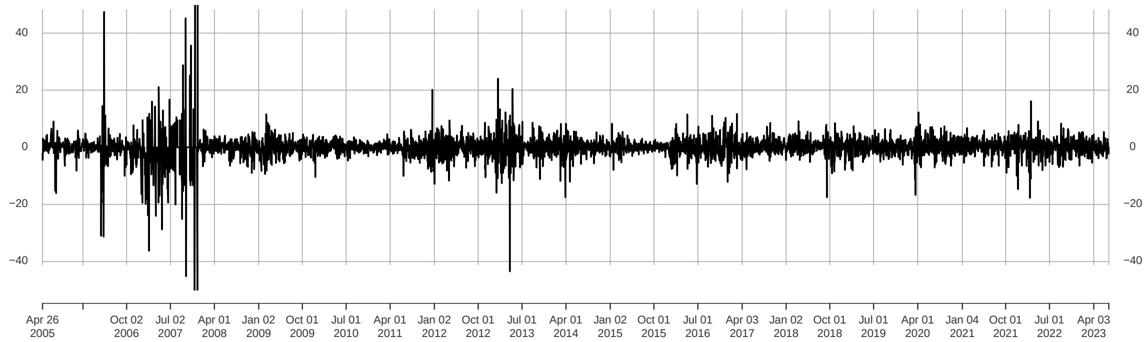

Figure 4: The daily log-returns on the carbon emissions futures.

the first phase of the EU ETS is the most prominent. Next, we test for the presence of autocorrelation and ARCH effects. Both null hypotheses that there is no time dependence in the first and second moments are rejected and we model them accordingly in two steps. First we estimate a mean model with both an intercept and an autoregressive coefficient. Then, we estimate the variance equations using an appropriate volatility model. More on the modelling procedure shall be discussed below.

The importance of carbon markets is increasing for several reasons. One crucial factor is their significance in achieving the Nationally Determined Contributions (NDCs) as outlined in the Paris agreement. As a result, global interest in carbon markets is on the rise, with approximately 83% of NDCs expressing a desire to utilize international market mechanisms to reduce GHG emissions. Negotiations regarding the implementation of such mechanisms have taken centre stage in meetings of the United Nations Framework Convention on Climate Change and ongoing discussions are slated to continue in future climate summits. Rising climate concerns as perceived by not only the media, but also the public, global investors and policymakers can cause volatility in carbon markets. Volatility of climate news drives comovements of volatilities of carbon-intensive asset prices. Campos-Martins and Hendry (in Press) showed that unexpected increases in concerns about the energy transition make oil and gas stock prices move globally. As a measure of concerns on carbon markets, we use the U.S. daily media climate change concerns index constructed by Ardia, Bluteau, Boudt, and Inghelbrecht (2022). We focus on the index specific to carbon markets whose most common words are *market, price, scheme, government, credit, euro, tonne, carbon, year, permit.* More generally, on any day, this index reflects both the percentage of risk words and the degree of negativity of the news articles published on that day by a specific source. The resulting article - and source - specific indices are aggregated to reflect the overall level of concerns and the fact that the impact of news does not tend to increase with time. For more details, we refer to Ardia, Bluteau, Boudt, and Inghelbrecht (2022). The index is available only through the end of August 2022. The 20-day average rolling window of the concerns index on carbon credit markets (CCM) is displayed in Figure 5. Concerns about carbon markets rise during climate summits, namely, COP12-Nairobi 2006, COP15-Copenhagen in 2009, COP21-Paris in 2015 and COP26-Glasgow in 2021. Albeit not steadily, we observe an increase in carbon markets concerns over time.

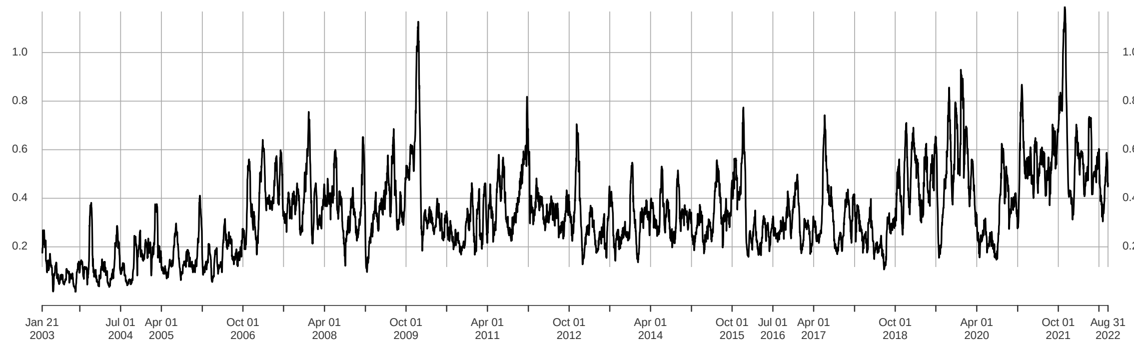

Figure 5: The daily media concerns index on carbon credit markets (20-day average rolling window).

We model the conditional mean of climate concerns in the same way as the log-returns on carbon futures. Having estimated both, we proceed to modelling the volatility equations. Since we suspect the underlying variance process to be nonstationary, we first test the null hypothesis of constant variance against a time-varying unconditional variance. The test is performed using the R package *tvgarch* (Campos-Martins and Sucarrat, 2023). Test results are summarised for the EU ETS carbon futures residuals and carbon markets concerns residuals in Tables 3 and 4, respectively. Outcomes of both non-robust and robust statistics are reported.

From the test results we conclude that both series show statistical evidence for time-varying unconditional volatility as the robust misspecification tests for the carbon futures and carbon markets residuals have p-values equal to 0.009 and 0.019, respectively. However, the corresponding results for the non-robust test statistics do not indicate any misspecification of the deterministic component for the EU ETS carbon future residuals whereas the carbon markets concerns residuals show evidence of misspecification. The test sequence

Table 3: Results from the sequential test of constant unconditional variance against a time-varying GARCH model applied to the EU carbon emissions futures residuals.

LM non-robust test	Test statistic	p-value
H_{0i}: $\phi_{i3} = \phi_{i2} = \phi_{i1} = 0$	6.236	0.101
H_{03i}: $\phi_{i3} = 0$	0.397	0.529
H_{02i}: $\phi_{i2} = 0 \vert \phi_{i3} = 0$	3.775	0.052
H_{01i}: $\phi_{i1} = 0 \vert \phi_{i3} = \phi_{i2} = 0$	2.066	0.151
LM robust test	Test statistic	p-value
H_{0i}: $\phi_{i3} = \phi_{i2} = \phi_{i1} = 0$	11.537	0.009
H_{03i}: $\phi_{i3} = 0$	0.409	0.522
H_{02i}: $\phi_{i2} = 0 \vert \phi_{i3} = 0$	2.528	0.112
H_{01i}: $\phi_{i1} = 0 \vert \phi_{i3} = \phi_{i2} = 0$	9.513	0.002

Table 4: Results from the sequential test of time-varying unconditional variance against a time-varying GARCH model applied to carbon markets concerns residuals.

LM non-robust test	Test statistic	p-value
H_{0i}: $\phi_{i3} = \phi_{i2} = \phi_{i1} = 0$	16.036	0.001
H_{03i}: $\phi_{i3} = 0$	0.209	0.648
H_{02i}: $\phi_{i2} = 0 \vert \phi_{i3} = 0$	3.709	0.054
H_{01i}: $\phi_{i1} = 0 \vert \phi_{i3} = \phi_{i2} = 0$	12.129	0.001
LM robust test	Test statistic	p-value
H_{0i}: $\phi_{i3} = \phi_{i2} = \phi_{i1} = 0$	9.939	0.019
H_{03i}: $\phi_{i3} = 0$	0.194	0.660
H_{02i}: $\phi_{i2} = 0 \vert \phi_{i3} = 0$	3.567	0.059
H_{01i}: $\phi_{i1} = 0 \vert \phi_{i3} = \phi_{i2} = 0$	5.604	0.018

for specifying the shape of the deterministic function g_{it} points towards $k_{i1} = 1$ since H_{01i} is more strongly rejected as H_{03i} and H_{02i}, suggesting that one location parameter seems to be the optimal number of thresholds for both series. Given the rejection of constant unconditional variance, we estimate a MTV-GARCH model with one transition function and one location of transition for each series. Graphs of the estimated long-term volatility component g_{it} are depicted in Figures 6 and 7 for the carbon futures and carbon markets concerns residuals, respectively. For illustration the estimated conditional variance of the GARCH model is also plotted in both graphs.

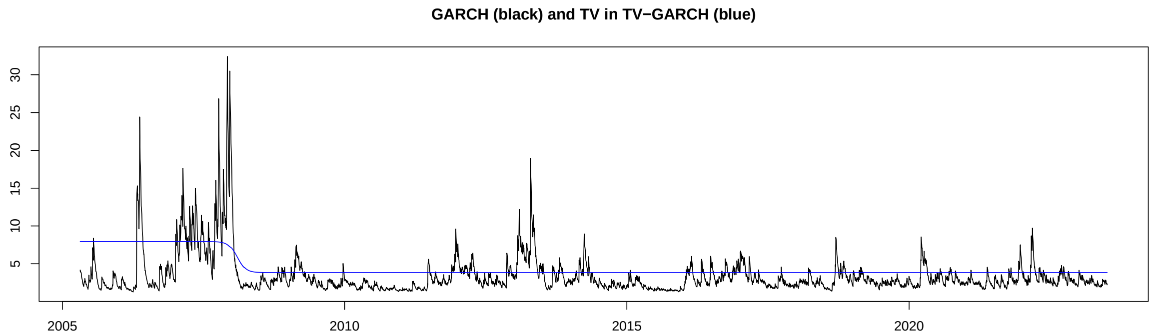

Figure 6: Estimated volatilities of the carbon futures residuals.

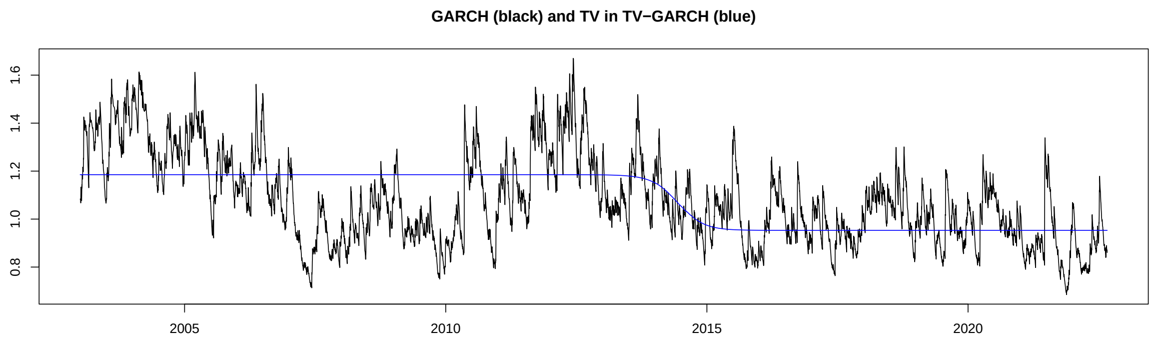

Figure 7: Estimated volatilities of the carbon markets concerns residuals.

We expect the unconditional variance of carbon futures returns to change over time as the design changes are introduced in the market. We also expect concerns about climate policies becoming more stringent and a disorderly transition more likely to cause further movements in the volatility of carbon futures returns. Therefore we apply the LM test of causality in variance proposed in this paper to the bivariate series. The test outcomes are

Table 5: Results from the univariate ($\rightarrowtail$) and multivariate ($\leftrightarrow$) tests of causality in variance under (mis-specified) constant unconditional variance.

	CEF $\rightarrowtail$ CCM		CCM $\rightarrowtail$ CEF		CEF $\leftrightarrow$ CCM	
	TR^2	p-value	TR^2	p-value	TR^2	p-value
Non-robust	1.556	0.212	0.115	0.734	1.671	0.434
Robust	3.678	0.055	0.152	0.696	3.830	0.147

Table 6: Results from the univariate ($\rightarrowtail$) and multivariate ($\leftrightarrow$) tests of causality in variance under time-varying unconditional variance.

	CEF $\rightarrowtail$ CCM		CCM $\rightarrowtail$ CEF		CEF $\leftrightarrow$ CCM	
	TR^2	p-value	TR^2	p-value	TR^2	p-value
Non-robust	1.079	0.299	2.837	0.092	3.916	0.141
Robust	0.906	0.341	0.024	0.877	0.930	0.628

available for both constant and time-varying unconditional variance. Results for either the non-robust and robust tests can be found in Tables 5 and 6.

These results are not only informative in themselves but also have an important implication. The robust test statistics indicate that an unmodelled nonstationary component of the variance could lead to spurious results, that is, under constant unconditional variance we would find supporting statistical evidence that climate concerns do not cause volatility of carbon futures. As the magnitude, direction and statistical significance of the causality in variance may change during the different phases of the EU ETS, we run the tests and estimate the volatility models shown above using a rolling window. Each covers 10 years of daily data for a total number of approximately 2500 observations in each window. The first window covers the years 2005-2014, the second 2006-2015, and so on and so forth until the last one corresponding to the years 2013-2022. In Table 7 and for each window we summarise in the second and third columns the results from the tests of constant unconditional variance, where the numbers shown indicate how many locations of transition are necessary to model the long-term component of the variance, in the fifth and six columns the results show if we find any statistical evidence of causality in the variance of carbon futures had we wrongly assumed stationary volatility (1 means that past squared values from another series causes volatility in the chosen series and 0 means no causality in variance) and, finally in the eight and ninth columns, present the same causality tests but having modelled nonstationarity in the variance accordingly. Each row

Table 7: Results from the rolling window test of constant conditional variance and tests of causality in variance.

	MTV-GARCH			GARCH-X			MTV-GARCH-X	
	CEF	CCM		CEF	CCM		CEF	CCM
2014	1	3	2014	0	1	2014	0	0
2015	1	3	2015	0	1	2015	0	0
2016	1	2	2016	0	1	2016	0	0
2017	0	2	2017	0	0	2017	0	0
2018	0	3	2018	0	0	2018	0	0
2019	1	1	2019	1	0	2019	1	0
2020	1	1	2020	0	0	2020	0	0
2021	0	1	2021	1	0	2021	1	0
2022	0	1	2022	1	0	2022	1	0

[1] *Notes:* In the second and third columns are reported the number of locations of transition necessary to model the long-term volatility component in the MTV-GARCH. In the fifth, six, eight and ninth columns the 1s mean that past squared values from another series cause volatility in the chosen series and 0s mean no causality in variance. Each row indicates the end year in the window.

indicates the end year in the window.

We also estimated the coefficients for the causal effects for different windows. The estimation results for the most recent window of observations (2013-2022) are presented below. All estimates were obtained using the R package *tvgarch* (Campos-Martins and Sucarrat, 2023). Robust standard errors are reported in parentheses. It is worth noting that for this subsample, the test of constant unconditional variance is only rejected for CCM (but not for CEF); see second and third columns of Table 7. We also find that past information from the CCM time series helps predict the variance of CEF, but not the other way around (see fifth and sixth columns of Table 7), and this causality in variance remains valid even after accounting for the nonstationary nature of the variance of CCM (see eight column of Table 7).

$$\begin{aligned}
\widehat{\sigma}^2_{\text{CEF},t} &= \underset{(0.065)}{0.045} + \underset{(0.025)}{0.121}\varepsilon^2_{\text{CEF},t-1} + \underset{(0.024)}{0.873}\widehat{\sigma}^2_{\text{CEF},t-1} + \underset{(0.054)}{0.117}\frac{\varepsilon^2_{\text{CCM},t-1}}{\widehat{g}_{\text{CCM},t-1}} \\
&\quad \text{Log-likelihood:} \ -6023.104 \qquad n = 2462 \\
\widehat{\sigma}^2_{\text{CCM},t} &= \widehat{h}_{\text{CCM},t} \times \widehat{g}_{\text{CCM},t} \qquad (59)
\end{aligned}$$

where

$$
\begin{aligned}
\widehat{h}_{\text{CCM},t} &= \underset{(0.146)}{0.522} + \underset{(0.028)}{0.119}\frac{\varepsilon^2_{\text{CCM},t-1}}{\widehat{g}_{\text{CCM},t-1}} + \underset{(0.155)}{0.360}\widehat{h}_{\text{CCM},t-1} \\
\widehat{g}_{\text{CCM},t} &= \underset{(-)}{0.906} - \underset{(0.052)}{0.346}\widehat{G}_1(\underset{(1.036)}{5.183}; \underset{(0.014)}{0.801}; t/T) \qquad (60) \\
& \text{Log-likelihood:} \ -3233.119 \qquad n = 2462.
\end{aligned}
$$

The estimated constant conditional correlation between the two series of standardized returns is 0.004, which is very close to zero. The estimated parameters and corresponding robust standard errors of the correlation structure of the MTV-EDCC-GARCH model are $\hat{a} = \underset{(0.028)}{0.031}$ and $\hat{b} = \underset{(0.850)}{0.273}$. The estimated dynamic conditional correlation (black) is depicted in Figure 8 alongside the constant conditional correlation (blue), for comparison. The low values of the estimated parameters in the DCC structure show low persistence and correlations oscillating erratically around the MTV-ECCC-GARCH model. Also, the conditional correlation of returns on carbon futures price and on the index of carbon markets media concerns seems to have remained very low over time.

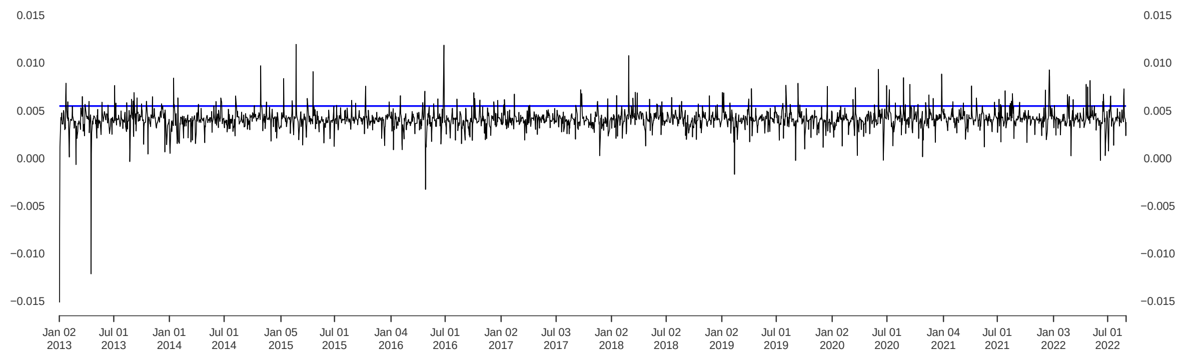

Figure 8: The dynamic conditional correlation (black) of carbon emissions future returns and changes in media concerns around carbon markets. The constant conditional correlation (blue) is also depicted for comparison.

The magnitude of the statistically significant causal effects have also changed over time as can be seen below. Changes in media concerns driven mostly by the coverage of the discussions and negotiations during climate summits seem to have driven volatility of carbon futures. The failure of COP25 in 2019 made it the longest COP in history at the time, as it extended nearly 44 hours past its scheduled end. During the conference, countries faced significant challenges in reaching agreements on crucial matters, including one of the top agenda items: providing guidance to ensure the integrity of international carbon markets. Specifically, there were difficulties in establishing consistent and robust accounting measures for emissions reductions transferred between nations. This effect of changes in media-based concerns on the volatility of carbon markets has been increasing over time as depicted in Figure 9.

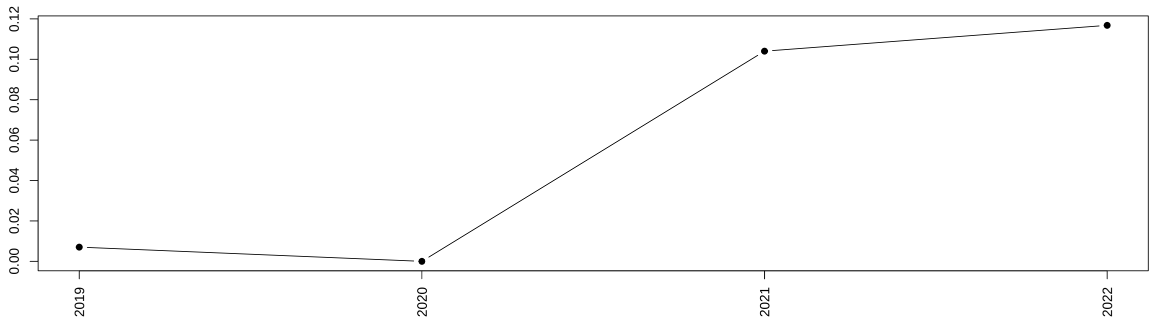

Figure 9: Causal effect of variance of media-based concerns on the variance of carbon futures returns.

8 Concluding remarks

In this paper we introduce a new multivariate conditional correlation GARCH model capable of describing the transmission mechanism of volatility spillovers across assets or markets. Yet recent literature has found that unaccounted shifts in the unconditional variance result in spurious volatility spillover effects and major estimation bias may be associated with model misspecification. Therefore, we generalize the multivariate time-varying GARCH model by Amado and Teräsvirta (2014) allowing for the presence of volatility transmission across assets or markets. The model is able to capture both short- and long-term movements of the volatility of returns by assuming a multiplicative decomposition structure where the past information of squared returns of all components are useful in predicting the variance process of any component.

As a misspecification test of the multivariate multiplicative time-varying GARCH model, we propose a new LM test for the presence of short-term volatility interactions. Specifically, we check the predictive power of past cross-asset (or cross-market) series information in the conditional variance component equation-by-equation. Monte Carlo simulations show that the robust test using auxiliary regressions has good size properties in finite samples although minor size distortions are observed in the multivariate version of the test statistic. The test has also reasonable power and the power of the test is an decreasing function with the persistence in volatility and correlation levels.

Our illustrative application using carbon emission futures and climate concerns suggests that if the nonstationary component of the variance was left unmodelled we would find no supporting statistical evidence for causality from past squared climate concerns returns in the variance of carbon futures returns. Causal effects of media-based concerns on future carbon markets are found to be statistically significant for most recent rolling periods.

For inference, we assume the estimators to be consistent and asymptotically normal. Asymptotic properties are known for some models nested in the general model proposed in this paper but they cannot be directly extended. We leave the asymptotic theory for future work. Another challenge when modelling variances and correlations is to evaluate how well the model reproduces the stylized facts of financial data and how good the model is for making predictions. Further work on misspecification tests may be helpful to provide some insight on this. After testing for modelling volatility transmissions among variables in the model one may further test for asymmetric ARCH effects on conditional volatility as another misspecification tool. Testing the adequacy of the correlation structure of a fitted MTV-ECC-GARCH model may be also a pertinent hypothesis test to carry out. These additional statistical tests can be developed in future extensions for model selection tool.

Appendix

See supplementary material.

References

Amado, C., and T. Teräsvirta (2013): "Modelling volatility by variance decomposition," *Journal of Econometrics*, 175, 142–153.

——— (2014): "Conditional correlation models of autoregressive conditional heteroscedasticity with nonstationary GARCH equations," *Journal of Business & Economic Statistics*, 32, 69–87.

——— (2017): "Specification and testing of multiplicative time-varying GARCH models with applications," *Econometric Reviews*, 36, 421–446.

Ardia, D., K. Bluteau, K. Boudt, and K. Inghelbrecht (2022): "Climate change concerns and the performance of green vs. brown stocks," *Management Science*, pp. 1–26.

Baillie, R. T., and T. Bollerslev (1990): "Intra-day and Inter-market volatility in foreign exchange rates," *Review of Economic Studies*, 58, 565–585.

Bauwens, L., C. M. Hafner, and D. L. Pierret (2013): "Multivariate volatility modeling of electricity futures," *Journal of Applied Econometrics*, 28, 743–761.

Bollerslev, T. (1990): "Modelling the coherence in short-run nominal exchange rates: A multivariate generalized ARCH model," *Review of Economics and Statistics*, 72, 498–505.

Campos-Martins, S., and D. Hendry (in Press): "Common volatility shocks driven by the global carbon transition," *Journal of Econometrics*.

Campos-Martins, S., and G. Sucarrat (2023): *tvgarch: Time varying GARCH modelling*R package version 2.4.1.

Caporin, M., and F. Malik (2020): "Do structural breaks in volatility cause spurious volatility transmission?," *Journal of Empirical Finance*, 55, 60–82.

Cifarelli, G., and G. Paladino (2005): "Volatility linkages across three major equity markets: A financial arbitrage approach," *Journal of International Money and Finance*, 24, 413–439.

Colacito, R., R. F. Engle, and E. Ghysels (2011): "A component model for dynamic correlations," *Journal of Econometrics*, 164, 45–59.

Conrad, C., and M. Karanasos (2010): "Negative volatility spillovers in the unrestricted ECCC-GARCH model," *Econometric Theory*, 26, 838–862.

Conrad, C., and M. Karanasos (2015): "Modelling the Link Between US Inflation and Output: The Importance of the Uncertainty Channel," *Scottish Journal of Political Economy*, 62, 431–453.

Engle, R. F. (1982): "Autoregressive conditional heteroskedasticity with estimates of the variance of United Kingdom inflation," *Econometrica*, 50, 987–1007.

——— (2002): "Dynamic conditional correlation: A simple class of multivariate generalized autoregressive conditional heteroskedasticity models," *Journal of Business & Economic Statistics*, 20, 339–350.

Ewing, B. T., and F. Malik (2005): "Re-examining the asymmetric predictability of conditional variances: The role of sudden changes in variance," *Journal of Banking & Finance*, 29, 2655–2673.

Feng, Y. (2006): "A local dynamic conditional correlation model," MPRA Paper 1592. Available at http://mpra.ub.uni-muenchen.de/1592.

Francq, C., and J.-M. Zakoïan (2012): "QML estimation of a class of multivariate asymmetric GARCH models," *Econometric Theory*, 28, 179–206.

Francq, C., and J.-M. Zakoïan (2016): "Estimating multivariate volatility models equation by equation," *Journal of the Royal Statistical Society Series B (Statistical Methodology)*, 78, 613–635.

Hamao, Y., R. W. Masulis, and V. Ng (1990): "Correlations in price changes and volatility across international stock markets," *Review of Financial Studies*, 3, 281–307.

He, C., and T. Teräsvirta (2004): "An extended constant conditional correlation GARCH model and its fourth-moment structure," *Econometric Theory*, 20, 904–926.

Hong, Y. (2001): "A test for volatility spillover with application to exchange rates," *Journal of Econometrics*, 103, 183224.

Jeantheau, T. (1998): "Strong consistency of estimators for multivariate ARCH models," *Econometric Theory*, 14, 70–86.

Karanasos, M., F. M. Ali, Z. Margaronis, and R. Nath (2018): "Modelling time varying volatility spillovers and conditional correlations across commodity metal futures," *International Review of Financial Analysis*, 57, 246–256.

Karanasos, M., A. G. Paraskevopoulos, F. M. Ali, M. Karoglou, and S. Yfanti (2014): "Modelling stock volatilities during financial crises: A time varying coefficient approach," *Journal of Empirical Finance*, 29, 113–128.

King, M. A., and S. Wadhwani (1990): "Transmission of volatility between stock markets," *Review of Financial Studies*, 3, 5–33.

Ling, S., and M. McAleer (2003): "Asymptotic theory for a vector ARMA-GARCH model," *Econometric Theory*, 19, 280–310.

Luukkonen, R., P. Saikkonen, and T. Teräsvirta (1988): "Testing linearity against smooth transition autoregressive models," *Biometrika*, 75, 491–499.

Silvennoinen, A., and T. Teräsvirta (2021): "Consistency and asymptotic normality of maximum likelihood estimators of a multiplicative time-varying smooth transition correlation GARCH model," *Econometrics and Statistics*, in press.

Song, P. X., Y. Fan, and J. D. Kalbfleisch (2005): "Maximization by parts in likelihood inference," *Journal of the American Statistical Association*, 100, 1145–1158.

Teräsvirta, T. (1998): "Modeling economic relationships with smooth transition regressions," in *Handbook of Applied Economic Statistics*, ed. by A. Ullah, and D. Giles. Dekker, New York.

Teräsvirta, T., D. Tjøstheim, and C. W. J. Granger (2010): "Modelling Nonlinear Economic Time Series," Oxford University Press, Oxford.

Wooldridge, J. M. (1990): "A unified approach to robust, regression-based specification tests," *Econometric Theory*, 6, 17–43.

Modelling causality in nonstationary variances with an application to carbon markets

Supplementary Material

Susana Campos-Martins*
Católica Lisbon School of Business & Economics

Cristina Amado†
University of Minho and NIPE

December 12, 2023

Abstract

This document contains supplementary material for the authors' article entitled "Modelling causality in nonstationary variances with an application to carbon markets". It consists of another empirical example to four major spot exchange rates to illustrate the usefulness of our procedure.

1 Application: Modeling exchange rate co-movements

First, we apply the test for causality in variance and the modelling strategy to exchange rate data. The data employed in the study are daily returns of four major spot exchange rates against the euro, among the most traded currencies, from the Bank of England Database. The return series are defined as 100 times the log-differences of the daily exchange rates of the USD, the JPY, the GBP and the AUD against the euro. The observation period starts in January 5, 1999 and ends in September 17, 2010, yielding a total of 2998 observations. Francq and Zakoïan (2012) studied the volatility comovements of the bivariate returns of the daily U.S. dollar and the Japanese yen exchange rates for the exact same period and three subperiods. Their results indicate that the volatility parameters appear to suffer from structural changes from one subperiod to another. The evidence of nonstationarity suggests that their constant conditional correlation asymmetric GARCH model may not be the most appropriate for fitting the data.

The graphs of the return series are depicted in Figure 1. At first, one may distinguish two different regimes in the JPY, GBP and AUD returns. A period of larger volatility at the beginning and the end of the sample period is observed in the series while for the period in between the volatility descends to a lower level. Identifying volatility regimes by visual inspection in the USD series is not so evident even though some extreme returns are also observed in the first and fourth quartiles.

Descriptive statistics, including conventional and robust measures of kurtosis and skewness, are reported in Table 1. The daily returns have approximately zero mean and

*Católica Lisbon School of Business & Economics, Palma de Cima, 1649-023 Lisbon, Portugal; e-mail address: scmartins@ucp.pt.

†Corresponding author: Department of Economics and NIPE, University of Minho, Campus de Gualtar, 4710-057 Braga, Portugal; e-mail address: camado@eeg.uminho.pt.

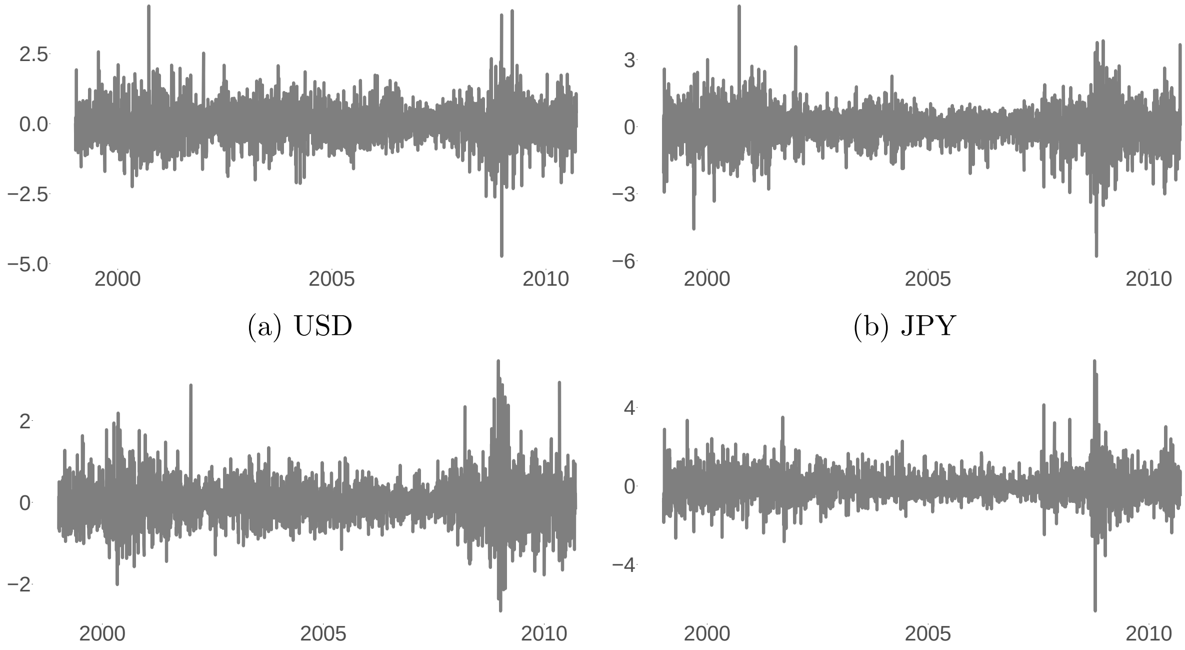

(a) USD (b) JPY

(c) GBP (d) AUD

Figure 1: Daily returns on the exchange rates of the U.S. dollar (USD), the Japanese yen (JPY), the British pound (GBP) and the Australian dollar (AUD) with respect to the euro from January 15, 1999 until September 17, 2010.

Table 1: Descriptive statistics

	Min.	Mean	Max.	Std. Dev.	Ex. Kurtosis	Rob. KR	Skewness	Rob. SK
USD	−4.735	0.003	4.204	0.667	2.767	0.173	0.108	0.009
JPY	−5.800	−0.006	5.396	0.814	3.949	0.121	−0.235	−0.043
GBP	−2.657	0.005	3.461	0.515	3.986	0.172	0.463	0.004
AUD	−6.370	−0.011	6.377	0.724	8.043	0.158	0.530	0.041

[1] *Notes:* Robust KR denotes the robust centred coefficient for kurtosis proposed by Moors (see Kim and White (2004)) and robust SK denotes the robust measure for skewness based on quantiles proposed by Bowley (see Kim and White (2004)).

are characterized by leptokurtosis and negative skewness. However, the robust measure of skewness is very close to zero suggesting that there is little skewness in the distribution of the returns. The robust measure of kurtosis is considerably smaller than the conventional measure, but it still suggests that there is excess kurtosis. This is clearly an indication of departures from normality in the distribution of returns. Diagnostic tests for time dependence and the Jarque-Bera test for normality are shown in Table 2. The corrected portmanteau statistics for serial correlation up to order 5 is not statistically significant suggesting that returns are serially independent but the Engle's LM test (Engle (1982)) for ARCH effects up to order 5 provide clear evidence that the squared returns are time dependent.

We first proceed with the modeling strategy described in Section 4 of the paper. After fitting a first-order GARCH model to capture the heteroskedastic behavior of the exchange rate returns, we apply the LM test for testing the null hypothesis of constant unconditional variance against a smoothly changing baseline volatility. The test results are presented in

Table 2: Results of the diagnostic tests for the daily returns

	non-rob. Q(5)	rob. Q(5)	ARCH(5)	JB
USD	3.751	3.185	39.71	962.1
	(0.586)	(0.671)	(0.000)	(0.000)
JPY	2.512	1.324	89.01	1976
	(0.775)	(0.932)	(0.000)	(0.000)
GBP	16.63	7.101	100.2	2092
	(0.005)	(0.213)	(0.000)	(0.000)
AUD	19.20	3.261	132.4	8222
	(0.002)	(0.660)	(0.000)	(0.000)

[1] *Notes:* The table reports test statistics for the non-robust (non-rob. Q(5)) and the corrected (rob. Q(5)) portmanteau test in the presence of ARCH effects proposed by Francq and Zakoïan (2009) up to order 5, the Engle's LM test (Engle (1982)) for ARCH effects up to order 5 (ARCH(5)) and the Jarque-Bera (JB) test. The numbers in parentheses are p-values.

the upper panel of Table 3. Only the outcomes of the robust statistics and corresponding p-values are reported. At each step of the testing sequence we halve the significance level of the test ($\tau = 0.5$). The null hypothesis of constant unconditional variance is rejected at the 5% significance level for the GBP, but it fails to reject the null of parameter constancy for the USD, JPY and AUD returns. However, there is evidence for rejection of constant long-term volatility against a single transition for JPY and AUD when testing with a second-order polynomial for the transition function as H_{02} is rejected at the 0.05 conventional level with p-values equal 0.038. The short test sequence for specifying the shape of the deterministic function g_{it} for the GBP returns points towards $k_{i1} = 2$, as H_{02} is rejected more strongly than the other hypotheses H_{01} or H_{03}.

After accounting for structural changes in the baseline volatility we test the hypothesis of an additive misspecification in the conditional variance for the returns using the test for causality in variance in Section 5 of the main paper. We apply the test to investigate the presence of volatility transmission from one exchange rate to another. The test results for the presence of short-term volatility interactions can be found in the middle panel of Table 3. They suggest that the volatility structure of the GBP returns is affected by, not only its own past information (known as an ARCH effect), but also by the past squared innovations of the remaining exchange rates (known as cross-market conditional heteroskedasticity effect) since the p-values are well below the 5% level. There is also statistical evidence that the volatility of the AUD returns is affected by the past squared innovations of the JPY series as the p-value equals 0.008. For the volatility of the JPY returns we identify insignificant volatility spillovers from past USD, GBP and AUD returns as the p-values are above the 5% level.

In order to examine causality in variance between the USD returns and the other exchange rates, we proceed to testing the presence of volatility spillovers under stationarity using the multivariate tests proposed by Pedersen (2017) and Nakatani and Teräsvirta (2009). The tests are based on the null hypothesis that there are no interactions between the volatility processes so that the ARCH and GARCH matrices are assumed as diagonal. The test statistics by Pedersen (2017) can be viewed as "corrected" versions of the test introduced by Nakatani and Teräsvirta (2009) when the true parameter vector is at the boundary of the parameter space. Results from the test statistic using auxiliary regressions proposed by Nakatani and Teräsvirta (2010) are reported in Table 4. Results from the Wald, Quasi Likelihood Ratio (QLR), Directed Lagrange Multiplier (LM_{D}) and standard

Table 3: Results from the sequence of robust tests of constant unconditional variance against a time-varying GARCH model and the test for causality in variance. Boldface indicates rejection of the null hypothesis at the 5% significance level.

	USD		JPY		GBP		AUD	
	Statistic	p-value	Statistic	p-value	Statistic	p-value	Statistic	p-value
Single transition								
LM_0	1.732	0.785	7.693	0.103	9.839	**0.043**	6.822	0.146
LM_{03}	0.123	0.725	0.726	0.394	0.660	0.417	0.052	0.820
LM_{02}	1.330	0.249	4.323	**0.038**	7.131	**0.008**	4.303	**0.038**
LM_{01}	0.313	0.855	1.960	0.375	2.003	0.367	1.775	0.412
Volatility interactions								
USD			2.380	0.123	7.983	**0.005**	2.604	0.107
JPY	–	–			5.523	**0.019**	6.936	**0.008**
GBP	–	–	3.326	0.068			1.565	0.211
AUD	–	–	2.551	0.110	4.271	**0.039**		
Double transition								
LM_0	–	–	7.512	0.111	20.72	**0.000**	9.564	**0.048**
LM_{03}	–	–	2.447	0.118	8.816	**0.003**	1.393	0.238
LM_{02}	–	–	1.489	0.222	1.180	0.277	0.232	0.630
LM_{01}	–	–	2.184	0.336	6.892	**0.032**	8.009	**0.018**

[1] *Notes:* The row headings LM_{01}, LM_{02} and LM_{03} report to the short test sequence of parameter constancy based on the first-order Taylor expansion of the transition function with $k_{ij} = 1, 2, 3$, respectively; see Amado and Teräsvirta (2017) for more details.

Table 4: Results from the bivariate tests of volatility spillovers. Boldface indicates rejection of the null hypothesis at the 5% significance level.

	USD−JPY		USD−GBP		USD−AUD	
	Statistic	p-value	Statistic	p-value	Statistic	p-value
Wald	3.152	0.398	29.11	**0.023**	23.24	**0.040**
QLR	3.529	0.372	43.22	**0.006**	28.56	**0.023**
LM_D	3.311	0.387	36.81	**0.011**	26.84	**0.028**
LM	1.620	0.805	15.51	**0.004**	8.251	0.083
non-rob. $\mathsf{TR}^2_{\mathrm{ECCC}}$	3.096	0.542	12.73	**0.013**	6.502	0.165
rob. $\mathsf{TR}^2_{\mathrm{ECCC}}$	3.861	0.425	12.48	**0.014**	6.811	0.146

[1] *Notes:* The table reports the test statistics and p-values for the Wald, QLR, LM_D and LM tests of Pedersen (2017) and the non-robust and robust $\mathsf{TR}^2_{\mathrm{ECCC}}$ tests of Nakatani and Teräsvirta (2010). The null hypothesis of a diagonal CCC-GARCH model is tested against the alternative of an ECCC-GARCH model.

Lagrange Multiplier (LM) test statistics discussed in Pedersen (2017) are also reported. The results suggest, based on the LM statistic, that there are no volatility spillovers between the currency pairs USD−JPY and USD−AUD as the p-values are not significant at any reasonable levels. This conclusion is in line with the findings of the test statistics by Nakatani and Teräsvirta (2009). In contrast, based on the W, QLR and LM_D tests, we reject the null hypothesis of no volatility spillovers for the pair USD−AUD as the statistics are all significant at the 5% level. The results also suggest strong causality in variance between the pair USD−GBP since the diagonality of the ARCH and GARCH matrices is strongly rejected by all test statistics at any reasonable levels.

To identify the direction for causality in variance we compute an equation-by-equation version of the $\mathsf{TR}^2_{\mathrm{ECCC}}$ test statistics by Nakatani and Teräsvirta (2010) (for the sake of saving space, these results are not reported). The LM tests suggest that the volatility from past GBP returns to USD returns is statistically significant at the 5% level and information coming to the market from past USD returns is also affecting the current volatility of the GBP returns. For the pairwise USD−AUD the univariate test results fail to reject the null hypothesis of no volatility spillovers in both directions. These results are consistent with the findings by the multivariate tests of Nakatani and Teräsvirta (2010). After fitting different GARCH models to the USD returns, we conclude that the best model is the GARCH model with GBP returns as predictor based on the Bayesian information criterion (BIC) of Schwarz (1978) and tentatively use it as the final model for the USD returns.

After modelling the variance equations to the data and before proceeding with estimation of the correlations, we test the possibility of g_{it} being also misspecified. Specifically, we check the necessity of an additional transition to capture the daily variation in the long-term volatility of JPY, GBP and AUD returns. The results from these misspecification tests are reported in the lower panel of Table 3. Fitting the MTV-ECCC-GARCH with one transition and testing for an additional transition for the GBP and AUD returns yields the p-values of 0.000 and 0.048 for the robust statistics, respectively. The short test sequence points towards $k_{i2} = 3$ for the GBP returns as H_{03} is more strongly rejected than the other hypotheses. For the AUD returns the test sequence suggests $k_{i2} = 1$. We tentatively assume these specifications for the deterministic component for currencies GBP and AUD.

Tables 5 and 6 report the estimation results for the volatility component of the MTV-ECCC-GARCH model for the deterministic and conditional variance components,

Table 5: Parameter estimates of the deterministic component for the exchange rate returns. Robust standard errors in parentheses.

	$\hat{\delta}_0$	$\hat{\delta}_1$	$\hat{\gamma}_1$	$\hat{c}_{11}$	$\hat{c}_{12}$	$\hat{\delta}_2$	$\hat{\gamma}_2$	$\hat{c}_{21}$	$\hat{c}_{22}$	$\hat{c}_{23}$
JPY	0.275 (–)	0.862 (0.146)	4.623 (–)	0.215 (0.013)	0.766 (0.020)					
GBP	5×10^{-5} (–)	0.296 (0.063)	4.743 (–)	0.203 (0.039)	0.768 (0.007)	0.237 (0.058)	3.742 (–)	0.169 (0.098)	0.570 (0.102)	0.916 (0.128)
AUD	5×10^{-5} (–)	0.811 (0.125)	2.525 (–)	0.345 (0.051)	0.987 (0.048)	0.440 (0.101)	5.495 (–)	0.730 (0.003)		

Table 6: Parameter estimates of the conditional variance component for the exchange rate returns. Robust standard errors in parentheses.

	$\hat{\omega}$	$\hat{\alpha}_{\text{USD}}$	$\hat{\alpha}_{\text{JPY}}$	$\hat{\alpha}_{\text{GBP}}$	$\hat{\alpha}_{\text{AUD}}$	$\hat{\beta}$	(4)	(3)	(2)	(1)
USD	0.002 (0.001)	0.027 (0.005)		0.012 (0.006)		0.962 (0.007)	0.995	0.995	0.997	0.997
JPY	0.034 (0.013)		0.067 (0.016)			0.899 (0.026)	0.966	0.966	0.966	0.997
GBP	0.038 (0.017)	0.033 (0.020)	0.015 (0.014)	0.045 (0.013)	0.004 (0.004)	0.883 (0.039)	0.922	0.935	0.974	0.995
AUD	0.073 (0.061)		0.034 (0.027)		0.073 (0.034)	0.816 (0.117)	0.889	0.929	0.957	0.993

[1] *Notes:* The table reports persistence for the CCC-GARCH model (1), the MTV-CCC-GARCH model (2), the MTV-ECCC-GARCH model with one transition function (3) and the MTV-ECCC-GARCH model with two transition functions (4).

respectively. By inspection of Table 5 the estimated values of the speed of transition are moderate indicating that the transitions from one volatility state to another are relatively smooth. The standard errors of the intercept and smoothness parameters are not available because δ_{ij} and $\mathbf{c}_{ij}$, $j = 1, ..., r_i$, are estimated conditionally on those parameters. Interestingly, the proximity of the estimates of the location parameters in the first transition function for the currencies JPY and GBP reveals a common long-term volatility pattern between the two exchange rates. This dynamics can also be seen from Figure 2. The baseline volatility starts decreasing in 2001 and remains low for a long period until the end of 2007, when it starts increasing again towards its initial level. Our findings suggest that the largest deterministic changes in the long-term volatility occur during recessions, namely, in the dot-com bubble, the subprime crisis and subsequent global financial crisis. A similar pattern is found for the AUD returns where the first transition is smoother than the second one. In order to evaluate how the slow (low-frequency) movements in the baseline volatility compare to the quick (high-frequency) movements obtained from an augmented GARCH (henceforth GARCH-X) process, we add the estimated volatilities from a GARCH$(1,1)$-X model to each panel of Figure 2. It is interesting to see how the baseline volatility follows the dynamics of the GARCH process as a smoothed conditional mean.

For comparison, in Table 6 are also reported the persistence levels for different estimated GARCH models, measured by the sum of the estimated ARCH and GARCH coefficients for the augmented GARCH model and by the eigenvalues (in decreasing order) of $\mathbf{A}_1 + \mathbf{B}_1$, where $\mathbf{A}_1$ and $\mathbf{B}_1$ are the ARCH and the GARCH matrices, respectively, for the extended GARCH model. From right to left, we show the volatility persistence estimated from the CCC-GARCH model, the MTV-CCC-GARCH model with one transition function, the MTV-ECCC-GARCH model with one transition function, and finally the MTV-ECCC-

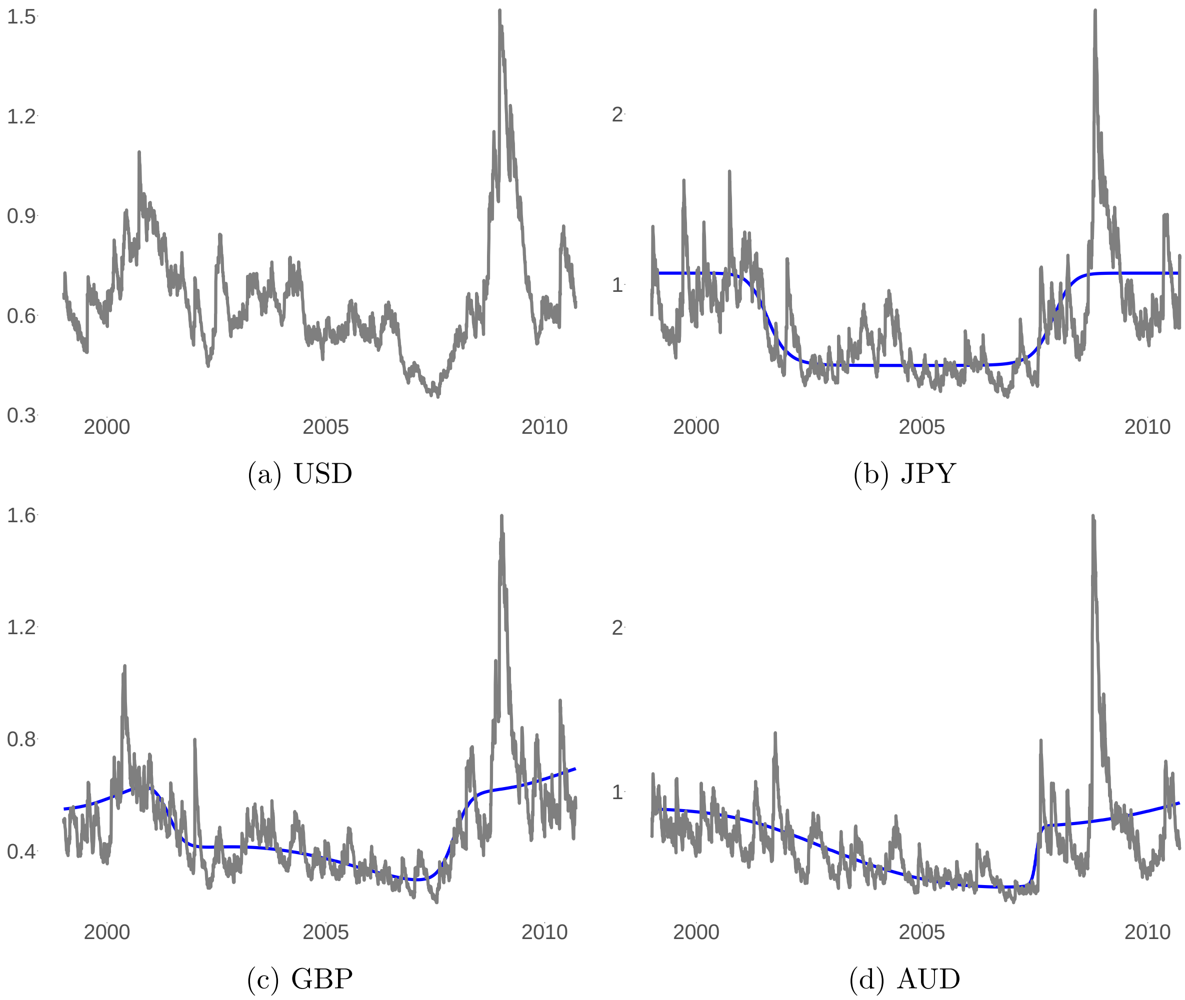

Figure 2: Volatilities from estimated augmented GARCH(1, 1)-X models (grey) and the estimated long-term volatilities defined by the g_{it} deterministic component (blue) for the currency returns.

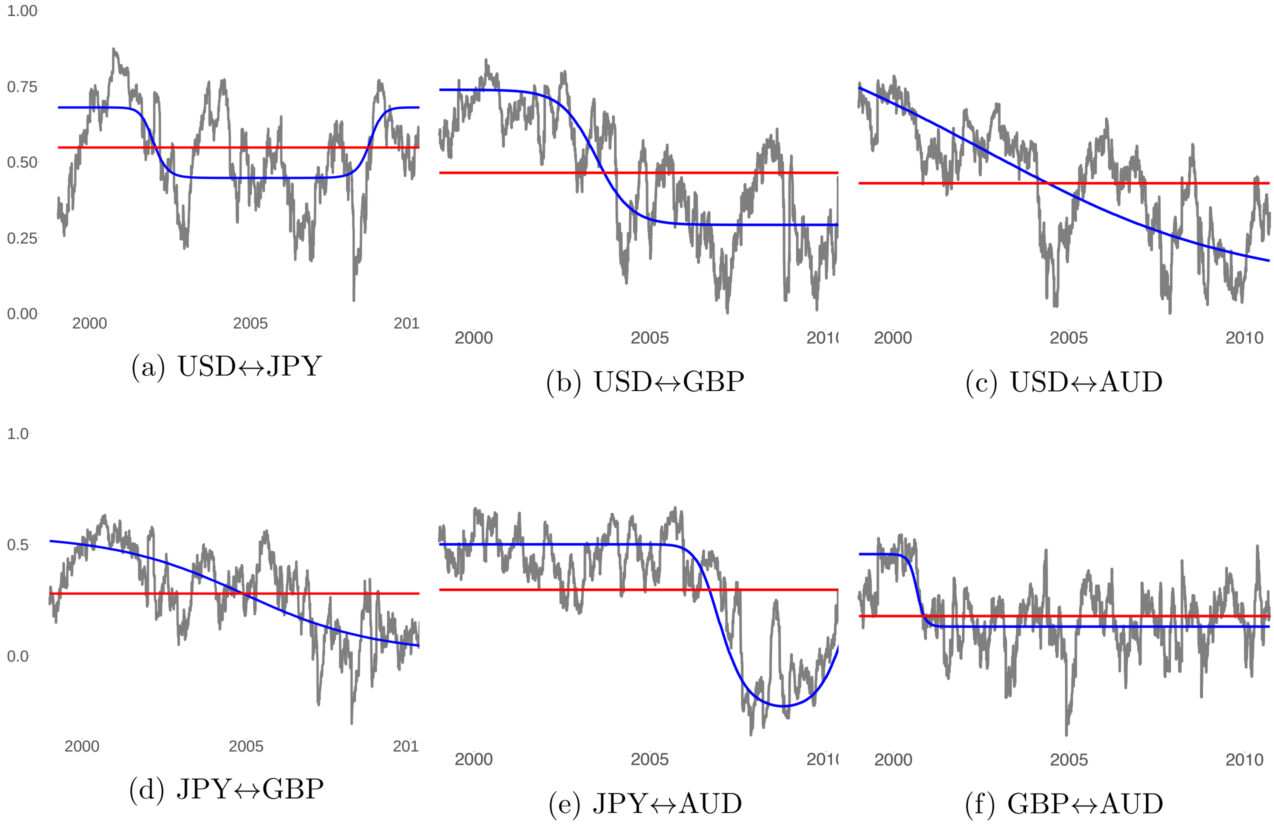

(a) USD↔JPY (b) USD↔GBP (c) USD↔AUD

(d) JPY↔GBP (e) JPY↔AUD (f) GBP↔AUD

Figure 3: The estimated constant conditional correlations (red), dynamic conditional correlations (grey) and the time-varying unconditional correlations (blue).

GARCH model with two transition functions. The model presented in column (4) is the final model fitted to the data. Interestingly, persistence decreases considerably by including cross-market conditional heteroskedasticity as predictors and/or rescaling the innovation series by the baseline volatility. Regarding the off-diagonal elements of the ARCH matrix, i.e., the variance interactions, we find a (statistically significant) bidirectional volatility transmission between the USD and GBP exchange rates.

After estimating the volatility component, we proceed with the estimation of the correlation models. In order to save space we only report plots of the correlation paths for each model. Panels in Figure 3 graph the estimated dynamic conditional correlations whose structure is defined in Equations (10)-(11) of the paper and the estimated deterministic unconditional correlations by Silvennoinen and Teräsvirta (2015) for bivariate models. For comparison, we also plot the level of constant conditional correlations between currency returns. The dynamic conditional correlations seem to fluctuate around the slower movement of correlations defined by the time-varying unconditional correlations. In general, the results show a downward trend in the correlations between exchange rate returns meaning that the co-movements tend to become weaker over time. Most of the transitions are gradual suggesting that these slow changes in co-movements are possibly due to market conditions between the currencies.

References

AMADO, C., AND T. TERÄSVIRTA (2017): "Specification and testing of multiplicative time-varying GARCH models with applications," *Econometric Reviews*, 36, 421–446.

ENGLE, R. F. (1982): "Autoregressive conditional heteroskedasticity with estimates of the variance of United Kingdom inflation," *Econometrica*, 50, 987–1007.

FRANCQ, C., AND J.-M. ZAKOÏAN (2009): "Bartlett's formula for a general class of nonlinear processes," *Journal of Time Series Analysis*, 30, 449–465.

FRANCQ, C., AND J.-M. ZAKOÏAN (2012): "QML estimation of a class of multivariate asymmetric GARCH models," *Econometric Theory*, 28, 179–206.

KIM, T.-H., AND H. WHITE (2004): "On more robust estimation of skewness and kurtosis," *Finance Research Letters*, 1, 56–73.

NAKATANI, T., AND T. TERÄSVIRTA (2009): "Testing for volatility interactions in the Constant Conditional Correlation GARCH model," *Econometrics Journal*, 12, 147–163.

NAKATANI, T., AND T. TERÄSVIRTA (2010): "An alternative test for causality in variance in the conditional correlation GARCH models," *mimeo*, Stockholm School of Economics.

PEDERSEN, R. S. (2017): "Inference and testing on the boundary in extended constant conditional correlation GARCH models," *Journal of Econometrics*, 196, 23–36.

SCHWARZ, G. E. (1978): "Estimating the dimension of a model," *Annals of Statistics*, 6, 461–464.

SILVENNOINEN, A., AND T. TERÄSVIRTA (2015): "Modeling conditional correlations of asset returns: A smooth transition approach," *Econometric Reviews*, 34, 174–197.

Most Recent Working Paper

NIPE WP 13/2023	**Susana Campos-Martins** and **Amado, C.**, Modelling causality in nonstationary variances with an application to carbon markets, 2023
NIPE WP 12/2023	Brekke, K. R., Dalen, D. M., and **Straume, O. R.** , Taking the competitor´s pill: when combination therapies enter pharmaceutical markets, 2023
NIPE WP 11/2023	**Cátia Cerqueira**, **Alexandre, F.**, and **Portela, M.**, Digitalization: the edge of first movers, 2023
NIPE WP 10/2023	Brekke, K. R., **Straume, O. R.**, and Sørgard, L., Trade, renewable energy, and market power in power markets, 2023
NIPE WP 9/2023	**António Pedro Coelho** and **Loureiro, G.**, Do Earnouts Create the Right Incentives?: Earnings Management Around Earnout-Based Acquisitions, 2023
NIPE WP 8/2023	**Fernando Alexandre**, Ferreira, D., Mendonça, S. and **Portela, M**. The elusive impact of R&D grants on firm productivity, 2023
NIPE WP 7/2023	Cirulli, V., Marini, G., Marini, M. A., and **Straume, O. R.,** Do Hospital Mergers Reduce Waiting Times? Theory and Evidence from the English NHS, 2023
NIPE WP 6/2023	**Rosa-Branca Esteves** and **Francisco Carballo-Cruz**, Can data openness unlock competition when an incumbent has exclusive data access for personalized pricing?, 2023
NIPE WP 5/2023	**Natália P. Monteiro** and **Odd Rune Straume**, Management, performance and pay, 2023
NIPE WP 4/2023	**Cristiana Gião** and **Rita Sousa**, Desenvolvimento de uma Matriz de Contabilidade Social para a análise do efeito das alterações climáticas no turismo, 2023
NIPE WP 3/2023	**Rosa-Branca Esteves** and Shuai, J., Behavior-Based Price Discrimination with a General Demand, 2023
NIPE WP 2/2023	**Rosa-Branca Esteves**, and Pasquier, N., Marketplace's incentives to promote a personalized pricing device: Does it pay-off to boost consumer disloyalty?, 2023
NIPE WP 1/2023	**João Cerejeira**, **Rita Sousa**, Bernardo, C. and Bento-Gonçalves, A., Do wildfires burn tourism intentions? The case of Portugal, 2023
NIPE WP 12/2022	**Luís Sá** and **Odd Rune Straume**, Hospital competition when patients learn through experience, 2022
NIPE WP 11/2022	**Cristina Amado**. Outlier Robust Specification of Multiplicative Time-Varying Volatility Models, 2022
NIPE WP 10/2022	Gabrielsen, T. S., Johansen, B. O. and **Odd Rune Straume**. Merger control in retail markets with national pricing, 2022
NIPE WP 09/2022	Liao, R. C. and **Gilberto Loureiro** and Taboada, A. G. Gender Quotas and Bank Risk, 2022
NIPE WP 08/2022	Hussain, T. and **Gilberto Loureiro**. Portability of Firm Corporate Governance in Mergers and Acquisitions, 2022
NIPE WP 07/2022	**Rosa-Branca Esteves**, Ghandour, Z., and **Odd Rune Straume**, Quality discrimination in healthcare markets, 2022
NIPE WP 06/2022	**Rosa-Branca Esteves**, The welfare effects of group and personalized pricing in markets with multi-unit buyers with a decreasing disutility cost in consumption, 2022
NIPE WP 05/2022	Kurt R. Brekke, Dag Morten Dalen and **Odd Rune Straume**, The price of cost-effectiveness thresholds, 2022
NIPE WP 04/2022	Pedro Luis Silva, **Carla Sá**, Ricardo Biscaia and Pedro N. Teixeira, High school and exam scores: Does their predictive validity for academic performance vary with programme selectivity?, 2022
NIPE WP 03/2022	Kurt R. Brekke, Dag Morten Dalen, **Odd Rune Straume**, Competing with precision: incentives for developing predictive biomarker tests, 2022
NIPE WP 02/2022	Wesley Mendes-da-Silva, Israel José dos Santos Felipe, **Cristiana Cerqueira Leal**, Marcelo Otone Aguiar, Tone of Mass Media News Affect Pledge Amounts in Reward Crowdfunding Campaign, 2022
NIPE WP 01/2022	**Rosa-Branca Esteves** and Jie Shuai, Personalized prices in a delivered pricing model with a price sensitive demand, 2022
NIPE WP 16/2021	**Rosa-Branca Esteves** and **Francisco Carballo Cruz**, Can data openness unlock competition when the incumbent has exclusive data access for personalized pricing?, 2021